

Western  Graduate&PostdoctoralStudies

Western University
Scholarship@Western

Electronic Thesis and Dissertation Repository

1-18-2013 12:00 AM

Investigating Adenosine's Role in Controlling the Cerebral Metabolic Rate of Oxygen following Hypoxia-Ischemia

Mustafa Ridha
The Univeristy of Western Ontario

Supervisor
Dr. Keith St. Lawrence
The University of Western Ontario

Graduate Program in Medical Biophysics
A thesis submitted in partial fulfillment of the requirements for the degree in Master of Science
© Mustafa Ridha 2013

Follow this and additional works at: <https://ir.lib.uwo.ca/etd>

 Part of the [Medical Biophysics Commons](#), [Medical Physiology Commons](#), and the [Physiological Processes Commons](#)

Recommended Citation

Ridha, Mustafa, "Investigating Adenosine's Role in Controlling the Cerebral Metabolic Rate of Oxygen following Hypoxia-Ischemia" (2013). *Electronic Thesis and Dissertation Repository*. 1100.
<https://ir.lib.uwo.ca/etd/1100>

This Dissertation/Thesis is brought to you for free and open access by Scholarship@Western. It has been accepted for inclusion in Electronic Thesis and Dissertation Repository by an authorized administrator of Scholarship@Western. For more information, please contact wlsadmin@uwo.ca.

**Investigating Adenosine's Role in Controlling the Cerebral Metabolic
Rate of Oxygen following Hypoxia-Ischemia**

(Thesis format: Monograph)

by

Mustafa Ridha

Graduate Program

in

Medical Biophysics

A thesis submitted in partial fulfillment

of the requirements for the degree of

Master of Science

The School of Graduate and Postdoctoral Studies

The University of Western Ontario

London, Ontario, Canada

© Mustafa Ridha 2012

THE UNIVERSITY OF WESTERN ONTARIO
School of Graduate and Postdoctoral Studies

CERTIFICATE OF EXAMINATION

Supervisor

Dr. Keith St. Lawrence

Supervisory Committee

Dr. David Lee

Dr. Dwayne Jackson

Examiners

Dr. Doug Fraser

Dr. Lisa Hoffman

Dr. Chris Ellis

The thesis by

Mustafa Ridha

entitled:

**Investigating Adenosine's Role in Controlling the Cerebral Metabolic Rate
of Oxygen following Hypoxia-Ischemia**

is accepted in partial fulfillment of the
requirements for the degree of

Master of Science

Date _____

Chair of the Thesis Examination Board

ABSTRACT

The cerebral metabolic rate of oxygen (CMRO₂) has been shown to be an early indicator of hypoxia-ischemia (HI); however, the mechanisms controlling post-HI CMRO₂ are not clear. One potential mechanism is the activation of the adenosine A₁ receptor due to increased adenosine concentrations during the insult. The present study investigated if the specific adenosine A₁ antagonist, DPCPX, would attenuate the typical reduction in CMRO₂ and electrical cortical activity following HI. Measurements of CMRO₂ and electrical cortical activity were obtained on piglets by near-infrared spectroscopy (NIRS) and amplitude-integrated electroencephalography (aEEG), respectively. The post-HI measurements of CMRO₂ and mean aEEG background voltage were significantly less depressed in piglets treated with DPCPX than controls (p <0.05). The significant difference in post-HI CMRO₂ and aEEG values between DPCPX-treated animals and controls suggests that the release of adenosine during HI leads to depressed cerebral energy metabolism due to the inhibition of neuronal activity.

Keywords:

Near-infrared spectroscopy, cerebral metabolic rate of oxygen, cerebral blood flow, hypoxic-ischemic encephalopathy, neonate, piglets, DPCPX, electroencephalography, adenosine, antagonist.

ACKNOWLEDGEMENTS

The work completed in this thesis would not have been possible without the gracious unconditional assistance of several individuals. First and foremost, I would like to thank my supervisor, Dr. Keith St. Lawrence, for his guidance, support and patience. I will forever be in debt to you for all that you have given to me. If I end up being half the researcher you are with your many, well-deserved, accolades and achievements, I will consider myself greatly blessed, thanks again. Secondly, I would like to thank my lab technicians; Jennifer Hadway, Lise Desjardins and Laura Morris for their limitless work-ethic which helped me tremendously to gather good results from my animal experiments. Also, a very special thanks to Ken Tichauer for teaching me so much and letting me continue on his legacy he left off before pursuing bigger and better opportunities. Last but certainly not least, a very warm thanks to Jonathon Elliot and Mamadou Diop, your wisdoms and knowledgeable support you have shared with me over the years were greatly appreciated. Financial support for the work described in this thesis was provided by the Heart and Stroke Foundation, without their assistance, none of this would be possible. Finally, I would like to thank all my friends and family for all of their unbridled support and patience over the many years. Degrees come and go but friends and family are forever.

TABLE OF CONTENTS

Certificate of Examination	ii
Abstract	iii
Acknowledgements	iv
List of Tables	vi
List of Figures	vi
List of Appendices	vii
List of Abbreviations	vii
CHAPTER 1– Introduction	1
1.1 Hypoxic-Ischemic Encephalopathy	1
1.2 Early Diagnosis and Prognosis	2
1.3 Biochemical Aspects	3
1.3.1 During Hypoxia-Ischemia	3
1.3.2 Reperfusion	4
1.4 Current Techniques for Detecting Compromised Brain Function	7
1.5 Near-Infrared Spectroscopy (NIRS)	8
1.5.1 Main Endogenous Chromophores	9
1.6 In-vivo Spectroscopy	12

1.7 Measuring Cerebral Blood Flow by NIRS.....	13
1.8 Cerebral Metabolic Rate of Oxygen.....	18
1.9 Assessing the Effects of HI on Cerebral Energy Metabolism by NIRS.....	19
1.10 Clinical Applications of NIRS in CBF and CMRO ₂ Measurements.....	21
1.11 Research Objective	23
CHAPTER 2 - METHODS & MATERIALS.....	25
CHAPTER 3 – RESULTS.....	30
CHAPTER 4 - DISCUSSION	37
CHAPTER 5 - SUMMARY.....	42
APPENDIX A	46
BIBLIOGRAPHY	52
CURRICULUM VITAE.....	61
LIST OF TABLES	
Table 3.1. – Group comparison of physiological variables.....	33
LIST OF FIGURES	
Figure 1.1 – Pathways associated with cell death in hypoxia ischaemia reperfusion.....	6
Figure 1.2 – Absorption spectra of endogenous chromophores	11
Figure 1.3 – Sample Arterial and Tissue ICG concentration curves	16
Figure 1.4 – Sample flow-scaled impulse residue function.....	17

Figure 3.1 – Group comparison of CBF, OEF and CMRO ₂	34
Figure 3.2 – Group comparison of mean aEEG and neural scores.....	35
Figure 3.3 – Group comparison of aEEG suppression delay.....	36

LIST OF APPENDICES

Appendix A – A near-infrared spectroscopy study to assess the effects of Indomethacin on cerebral blood flow and metabolic rate of oxygen in preterm infants.....	46
---	----

LIST OF ABBREVIATIONS

AD	Adenosine
ADP	Adenosine Diphosphate
aEEG	Amplitude Integrated Electroencephalography
ATP	Adenosine Triphosphate
Ca ²⁺	Calcium Cation
CBF	Cerebral Blood Flow
CBV	Cerebral Blood Volume
Cl ⁻	Chlorine
CMRO ₂	Cerebral Metabolic Rate of Oxygen
CSvO ₂	Cerebral Venous Oxygen Saturation
DDG	Dye Densitometer
DPCPX	8-Cyclopentyl-1,3-dipropylxanthine
EEG	Electroencephalography

HbA	Hemoglobin Alpha 1
HbF	Fetal Hemoglobin
HbO ₂	Oxy-Hemoglobin
HHb	Deoxy-Hemoglobin
HI/E	Hypoxia-Ischemia/Encephalopathy
ICG	Indocyanine Green
i/nNOS	Inducible/Neuronal Nitric Oxide Synthase
IRF	Impulse Residue Function
K ⁺	Potassium
MAP	Mean Arterial Pressure
MRS	Magnetic Resonance Spectroscopy
MTT	Mean Transit Time
N ₂ O	Nitrous
NaOH	Sodium Hydroxide
NIRS	Near-infrared Spectroscopy
NICU	Neonatal Intensive Care Unit
NMDA	N-Methyl-D-Aspartate
NO	Nitric Oxide
O ₂ ⁻	Super Oxide
OEF	Oxygen Extraction Fraction
pCO ₂	Partial pressure of Carbon Dioxide
PCr	Phosphocreatine

PET	Positron Emission Tomography
pO ₂	Partial pressure of Oxygen
ROS	Radical Oxygen Species
S _a O ₂	Arterial Oxygen Saturation
S _v O ₂	Venous Oxygen Saturation
SE	Standard Error
SPECT	Single-Photon Emission Computed Tomography.
tHb	Total Hemoglobin

CHAPTER 1

1.1 Hypoxic-Ischemic Encephalopathy

Perinatal cerebral hypoxic-ischemic encephalopathy (HIE) is the leading cause of brain injury in term newborns [1]. Cerebral HIE is defined as an acute reduction in the delivery of oxygen and blood flow to the brain [2]. Approximately 1 out of every 500 term newborns are diagnosed with HIE and, of those, 15 to 20% will not survive past the neonatal period. Of the survivors, up to 25% will have significant neurological deficits including cerebral palsy, mental retardation and epilepsy [2, 3]. Perinatal HIE is primarily associated with events during labor/delivery such as breech extractions, rotational maneuvers, prolonged labor, and acute placental or cord disturbances. These events result in a loss of cerebral vascular autoregulation, leading to insufficient cerebral blood flow and ultimately brain injury, depending on the duration and severity of the ischemic insult [4].

The onset of hypoxia ischemia (HI) does not bring forth immediate brain injury, rather, there is a delay of approximately 12 to 72 h before any evidence of brain injury manifests [5]. The realization of this delay has led to the idea that early interventions (i.e. hypothermia [6]) during this period could improve neurological outcome and, consequently, the delay is often termed the “therapeutic window” [4, 7, 8]. Unfortunately, early detection of brain injury in newborns by clinical signs (discussed in the following section) can be subtle or manifest after the therapeutic window [7, 9].

The remaining sections of the chapter will discuss techniques for early detection of HI in newborns, the biochemistry of HI in early and late phases after onset, and the connection to brain injury. The chapter will then shift focus to discuss near-infrared spectroscopy (NIRS) and the techniques developed to measure cerebral blood flow (CBF) and the cerebral metabolic rate of oxygen (CMRO₂). This section will be followed by a review of previous studies investigating post-HI changes in cerebral energy metabolism, its relationship to brain injury, and the potential mechanisms controlling CMRO₂ during the reperfusion phase. The chapter will end with an overview of clinical studies of NIRS applied to the newborn, which is the focus of the appendix.

1.2 Early Diagnosis and Prognosis

Current methods employed for diagnosis of HIE in newborns are limited due to the delicate nature of neonatal neurology/physiology. The most commonly used indicator of birth asphyxia is heart rate abnormality. It has been reported that abnormal fetal heart rate at birth is well correlated with neurological outcome at 1 year [10]; however, in other cases abnormal heart rate patterns showed no correlation with cognitive functions [11]. This difference supports the idea of a natural resiliency in newborns through endogenous protectors (such as oligotrophins) against cell death [12]. Other diagnostic techniques for assessing HI include low-extended APGAR/SARNAT scores, the need for resuscitation in the delivery room, and evidence of severe fetal acidemia [13]. All of these techniques suffer from poor

specificity and a more precise method of diagnosis of perinatal HI is needed to avoid unnecessary treatment of healthy newborns [14].

1.3 Biochemical Aspects

To understand the clinical relevance of HIE, we need to investigate its pathophysiology, particularly how it affects cerebral metabolism, hemodynamics, biochemistry, and tissue viability.

1.3.1 During Hypoxia-Ischemia

Hypoxia-ischemia is usually initiated by a reduction in oxygen (i.e., hypoxia), with the onset of ischemia occurring after the loss of autoregulation (i.e. the inability of the cerebral vasculature to maintain adequate CBF during systemic hypotension). Because of the lack of sufficient oxygen delivery, HI is typically accompanied by a compensatory increase in an oxygen independent energy production via anaerobic glycolysis and the consumption of high-energy phosphates, such as phosphocreatine (PCr) [15]. However, these alternate energy sources are not sufficient to satisfy energy demands, resulting in a depletion of adenosine triphosphate (ATP).

Insufficient ATP production will adversely affect many cellular mechanisms. Of major importance are those processes responsible for cell integrity/structure by controlling proper ion balance, primarily Na^+ , Cl^- and Ca^{2+} . Inadequate energy supply results in a large influx of these ions into the cells (efflux of potassium and sodium ions, an influx of calcium), leading to cellular edema and lysis. The fraction of cells

that will undergo irreversible membrane injury will ultimately depend on the severity and duration of HI [8]. In addition, this influx of Ca^{2+} is believed to initiate other mechanisms – in particular, the destruction of mitochondrial integrity leading to the formation of radical oxygen species (ROS) [8] – that ultimately leads to further cellular damage during the reperfusion phase.

1.3.2 Reperfusion

The return of normal blood flow and oxygen levels to the brain triggers immediate actions that attempt to restore cellular homeostasis. ATP and PCr levels are gradually replenished by the return of oxidative metabolism; however, there is evidence that mitochondrial function is impaired following HI. Studies have shown that mitochondrial impairment, including depressed respiration, is still occurring 6 h after HI [16-18]. One study involving a neonatal rat model demonstrated suppressed mitochondrial respiration up to a few days after HI [17].

Mitochondrial dysfunction is known to play a pivotal role in neurodegeneration during the reperfusion phase by initiating and being a target of oxidative stress [19, 20]. This effect is greatly exasperated by elevated NO levels, which combines with O_2^- to form the highly toxic agent peroxynitrite and inhibits mitochondrial respiration [17, 18]. Despite its short half-life, peroxynitrite is able to rapidly diffuse across cell membranes and affect surrounding cells [20]. It also inactivates enzymes including mitochondrial ATPase, inhibiting mitochondrial electron transport, which leads to cells inability to sustain homeostasis and eventually apoptosis [21] (Figure 1).

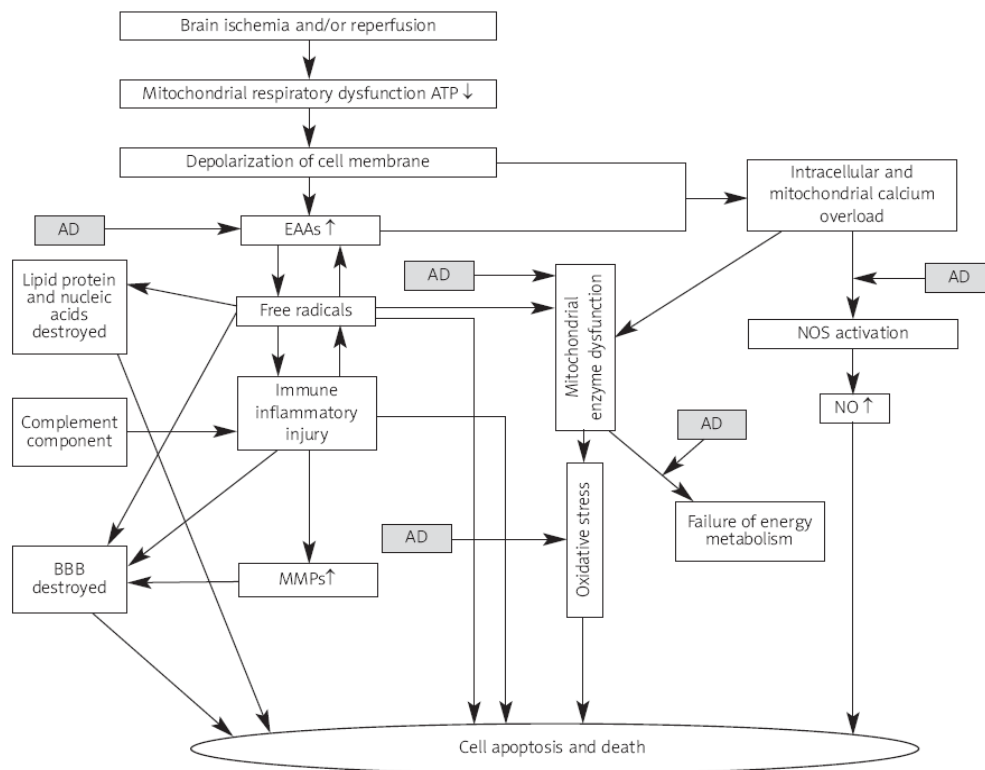
Another major event in the neurotoxic cascade during reperfusion is the release of glutamate. Excessive glutamate opens N-methyl-D-aspartate (NMDA) receptors causing cells to flood with calcium (Ca^{2+}). Increased Ca^{2+} activates inflammatory mediators, generates reactive oxygen species, and increases neuronal and inducible nitric oxide synthase (nNOS/iNOS), all of which lead to protein and DNA damage and oxidative degradation of lipids. This begins a chain reaction as ROS, lipid degradation and NO all enhance glutamate release, leading to further influxes of Ca^{2+} in a vicious cycle that ultimately leads to mitochondrial cell death [22]. The administration of an NMDA receptor antagonist has been shown to improve mitochondrial respiration and reduce brain injury [23]. The evidence that mitochondrial impairment precedes delayed brain injury suggests that assessing mitochondrial function could be used as an early marker of ensuing cellular damage [16].

These damaging pathways set forth a biochemical cascade leading to cell death, which usually occurs between 24 and 48 h after HI. Delayed brain injury is associated with the onset of secondary energy failure as characterized by a crash in high-energy metabolites despite normal levels of arterial oxygen saturation, blood pressure and blood glucose [24, 25]. It is also associated with seizure activity and inflammatory responses [25]. Ultimately, these events lead to mitochondrial swelling, release of pro-apoptotic proteins, and cell death [26]. Since the cerebral metabolic rate of oxygen reflects mitochondrial energy production, it could be used to detect compromised brain function before the onset of secondary energy failure. The

following section will discuss techniques for detecting altered cerebral energy metabolism during the critical early reperfusion phase.

Figure 1.1- Pathways associated with cell death in hypoxia ischaemia reperfusion

[8]



1.4 Current Techniques for Detecting Compromised Brain Function

Evidence of impaired cerebral energy metabolism following HI has been reported in studies using magnetic resonance spectroscopy (MRS) and electroencephalography (EEG) [27, 28]. With MRS, an increase in lactate concentration during early reperfusion correlates with insult severity [29-31], presumably indicating increased anaerobic metabolism. However, the early lactate peak is transient and has been found to suffer from poor specificity [31]. Magnetic resonance spectroscopy has also been used to confirm the causal relationship between impaired oxidative metabolism and delayed brain injury, as evident by the progressive decline in high-energy phosphates and the concurrent increase in lactate [15, 24, 32]. However, these changes are not observed until late in the reperfusion period – i.e., after the therapeutic window. A practical limitation with using MRS for diagnosis of HIE is the need to transport the newborn to the imaging suite, which may not be feasible depending on the condition of the patient.

Amplitude-integrated encephalography (aEEG) is increasingly being used in neonatal intensive care units (NICU) for continuous monitoring of cerebral electrical activity in critically ill newborns [28, 33]. The presence of hypoxic-ischemic injury can be determined by specific EEG patterns, including burst suppression, very low voltages, and an isoelectric/flat trace [34-39]. The limitation of aEEG for early diagnosis of abnormal brain energy function stems from its poor sensitivity [40]. Normal EEG activity has been documented in newborns with clinical evidence of

brain death [41] and, conversely, newborns can present a flat trace EEG signal in the first hours after HI and yet continue to develop normally [41].

The lack of current clinical techniques to diagnose HI within the therapeutic window has created a need for newer techniques capable of accurately detecting the onset and severity of brain insult within the critical first hours following birth. The strong correlation between mitochondrial dysfunction and insult severity suggests that a non-invasive measure of the cerebral metabolic rate of oxygen ($CMRO_2$) could improve early prognosis of HIE. The interest in NIRS stems from its portability, which enables bedside monitoring, and its sensitivity to blood oxygenation, which can be related to the energy demands of tissue. Section 1.8 will discuss how $CMRO_2$ can be measured by near-infrared spectroscopy (NIRS). This section will be followed by review of previous studies using NIRS to assess the effects of HI on cerebral energy metabolism. The last section is a discussion on clinical studies using NIRS to measure $CMRO_2$ in newborns.

1.5 Near-Infrared Spectroscopy (NIRS)

The relative transparency of tissue to near-infrared light (700-1000 nm), coupled with the unique absorption properties of oxy and deoxy hemoglobin (HbO_2 and HHb , respectively) enable tissue blood oxygenation to be assessed by NIRS [42]. The concentration of endogenous light absorbers, which are referred to as chromophores, can be determined by the loss of light intensity as light passes through tissue. Ignoring for the moment the scattering of light in tissue, the change in light

intensity can be related to the concentration of a chromophore by the Beer-Lambert Law:

$$A = \log\left(\frac{I_0}{I}\right) = \varepsilon CL \quad (1.1)$$

where A is the absorption of light as it passes through the medium, C is the chromophore concentration in the medium, ε is the specific extinction coefficient of the chromophore, and L is the physical distance that the light travelled. Absorption is defined as the log of the ratio of light intensity emitted (I_0) to the intensity detected (I). Equation 1.1 can be expanded to account for multiple chromophores, each with its own specific extinction coefficient:

$$A(\lambda) = L \sum_{i=1}^n \varepsilon_i(\lambda) C_i \quad (1.2)$$

where λ is wavelength, ε_i is the specific absorption of the i^{th} chromophore, and C_i is the concentration of the i^{th} chromophore. The concentration of each can be determined by acquiring absorption measurements at multiple wavelengths.

1.5.1 Main Endogenous Chromophores

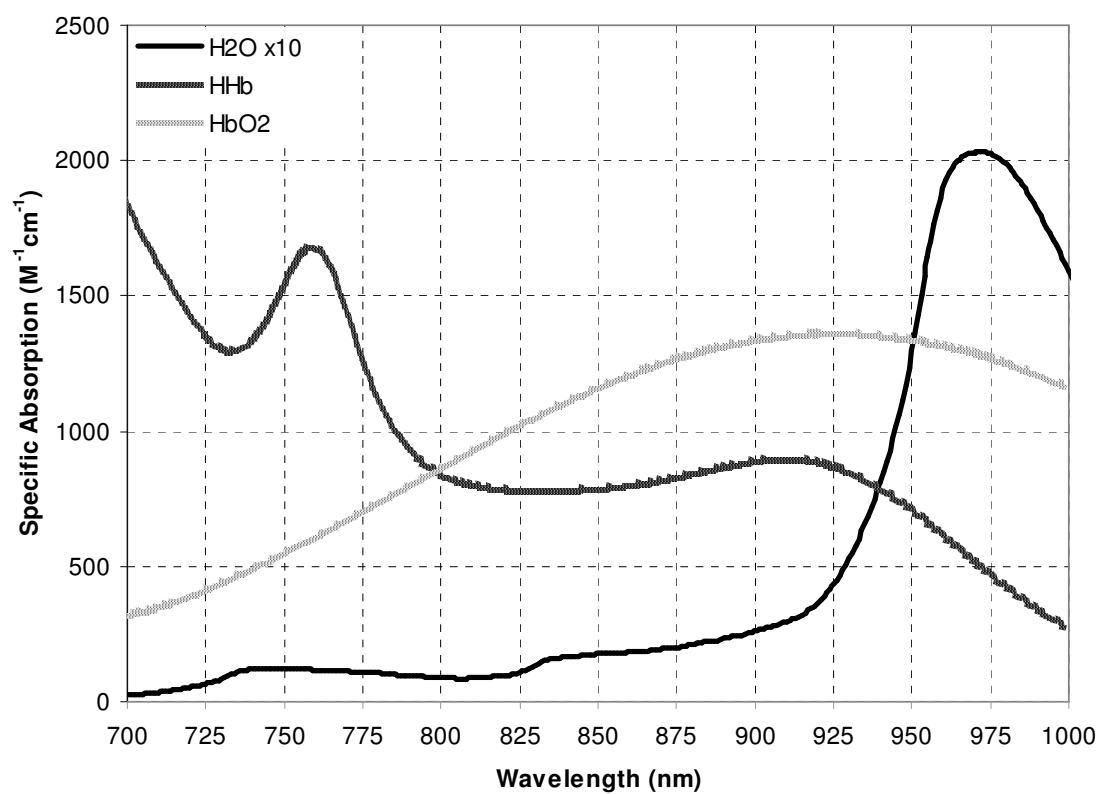
Although water is a weak absorber of NIR light, its contribution to the overall absorption is significant because of its large abundance in tissue: 80% in the adult brain and 85% in the newborn brain [43]. The high absorption of water at wavelengths greater than roughly 1000 nm sets the upper limit of the NIR spectrum for probing biological tissue [44]. There are three distinct absorption peaks for water

within the NIR range at 740, 840 and 925 nm. Although water absorption has not received nearly the attention of hemoglobin in NIRS studies, its stable concentration in tissue, particularly brain, and its unique absorption features provides a unique method of quantifying NIRS measurements, as will be discussed in section 1.7.

Of all of the endogenous NIR chromophores, hemoglobin has the largest attenuation peak due to its high absorption and concentration [44, 45]. The two most common forms of hemoglobin are hemoglobin alpha (HbA) and fetal hemoglobin (HbF). The latter is found in newborns; however, its specific absorption spectrum is the same as HbA. The physiological and clinical interests in NIRS primarily stems from the unique absorption spectra of HHb and HbO₂ (Figure 1.2). By acquiring measurements at multiple wavelengths, the difference in absorption spectra between HHb and HbO₂, provides a means of determining each concentration, from which tissue oxygenation extraction (fraction) (OEF) can be determined:

$$OEF = \frac{([Hb]_v - [Hb]_a) * 1.39 \text{ ml} \frac{O_2}{gHb}}{[\text{Arterial } O_2]} \quad (1.3)$$

Analogous to the upper limit placed by water, the strong absorption of hemoglobin at wavelengths below 600 nm sets the lower limit of the biological window.

Figure 1.2–Absorption spectra of endogenous chromophores

The absorption spectra of water (H₂O), deoxy-hemoglobin (HHb), and oxy-hemoglobin (HbO₂) within the near-infrared range.

1.6 In-vivo Spectroscopy

In 1977 the first *in vivo* study demonstrating the sensitivity of NIRS to brain oxygenation was performed in an animal model by Jobsis *et al.* [42]. Subsequent studies extended this method to human adults [46] and newborn infants [47]. However, the main challenge to *in vivo* spectroscopy is light scattering. Scattering in tissue disperses and diverges the transmitted light, reducing the intensity that can be detected. Scattering has wavelength dependence and alters the linear relationship between light absorption and the concentration of the chromophores. One method for characterizing the effects of light scattering in tissue is to modify the Beer-Lambert Law to account for the non-linear path that scattered light takes through tissue:

$$A(\lambda) = \beta(\lambda)\varepsilon_i(\lambda)C_i + G(\lambda) \quad (1.4)$$

where β is called the differential pathlength which is much greater than the physical distance between the light source and detector due to light scattering. The additional factor G accounts for the attenuation of light in tissue due to scattering [48]. This equation demonstrated that measuring chromophores' concentrations requires removing the effects of losses in absorption due to scattering and determining the differential pathlength.

The work presented in this thesis uses a NIRS technique referred to as second derivative spectroscopy to quantify the concentrations of chromophores, as described by Matcher *et al.* [44]. Second derivative NIRS relies on the principle that both β and G have a weak dependence on wavelength. Therefore, if the second derivative of

equation 1.4 is taken with respect to wavelength, G and any derivative terms with respect to β will disappear, leaving:

$$\frac{\partial^2 A(\lambda)}{\partial \lambda^2} = \beta(\lambda) \sum_i \frac{\partial^2 \varepsilon_i(\lambda)}{\partial \lambda^2} C_i \quad (1.5)$$

Assuming a constant water concentration, the mean pathlength can be determined using the water features at 740 and 840 nm. Since the HHb absorption spectrum has a strong characteristic at 770 nm, the water-derived differential pathlength can be used to calculate the absolute concentration of HHb. This approach is reasonable in the brain because the water concentration is extremely stable and only changes a few percent, even after HI [49]. The second main assumption of this technique is that the tissue volume interrogated is homogeneous, which is reasonable for newborns since the skull and scalp are relatively thin compared to adults.

1.7 Measuring Cerebral Blood Flow by NIRS

Cerebral blood flow (CBF) can be measured by NIRS by tracking the uptake of a blood flow tracer into brain tissue. The initial approach used a small transient change in arterial oxygenation as an endogenous (HbO₂) tracer [44, 50-53], and it has been validated by comparison with CBF measurements obtained with the ¹³³Xenon tracer clearance technique [54]. However, this method is limited by its poor precision and sensitivity [50]. An alternative approach is to use the light absorbing dye, indocyanine green (ICG), as an exogenous contrast agent. Indocyanine green is a water-soluble tricyanocyanine dye that is strongly protein bound (95%) in blood and

has a relatively short biological half-life (~5 min). The dye has a unique absorption spectrum with a peak absorbance around 800 nm. When injected into the blood stream, it rapidly binds with plasma proteins (albumin or lipoproteins), causing a shift in its absorption spectrum with a new peak at 805 nm [55]. The first use of ICG for an NIRS application was by Colacino *et al.* to study cerebral hemodynamics in ducks [54]. Indocyanine green has a high safety record in human applications [56-61]. Hope-Ross *et al.* conducted a safety study of 3149 adult patients suffering from ophthalmia [62]. They reported that the frequencies of mild, moderate and severe side effects were 0.15%, 0.2% and 0.05%, respectively. The first application involving human newborns was by Patel *et al.* [63], who compared the SO_2 manipulation and ICG methods of measuring CBF in newborns, and demonstrated a strong correlation between the CBF values determined by the two techniques ($r = 0.93$). However, the requirement of rapid changes in arterial oxygen saturation is difficult to achieve in newborns. For the HbO_2 method, 45% of the measurements collected did not meet the quality criteria and had to be neglected, as opposed to only 11% for the ICG technique. This is related to the greater precision observed with the ICG method: 85%, compared to 76% for HbO_2 .

Cerebral blood flow and other hemodynamic parameters, cerebral blood volume (CBV) and mean transit time (MTT) can be determined by monitoring the dynamic change in the brain concentration of ICG following an intravenous bolus injection [64]. With this approach, which is analogous to dynamic contrast-enhanced techniques used with computed tomography and magnetic resonance imaging [65],

the time-varying concentration of ICG in brain is modeled as a linear time-invariant system:

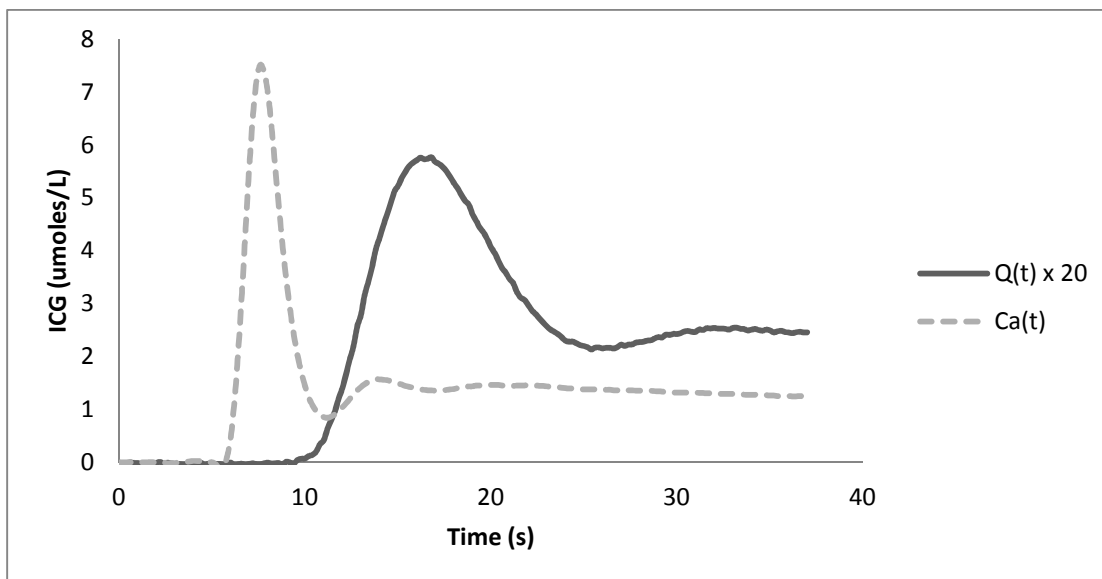
$$Q(t) = F \int_0^t C_a(u)R(t-u)du \quad (1.6)$$

This equation is more commonly written in its condensed form:

$$Q(t) = F \cdot C_a(t) * R(t) \quad (1.6b)$$

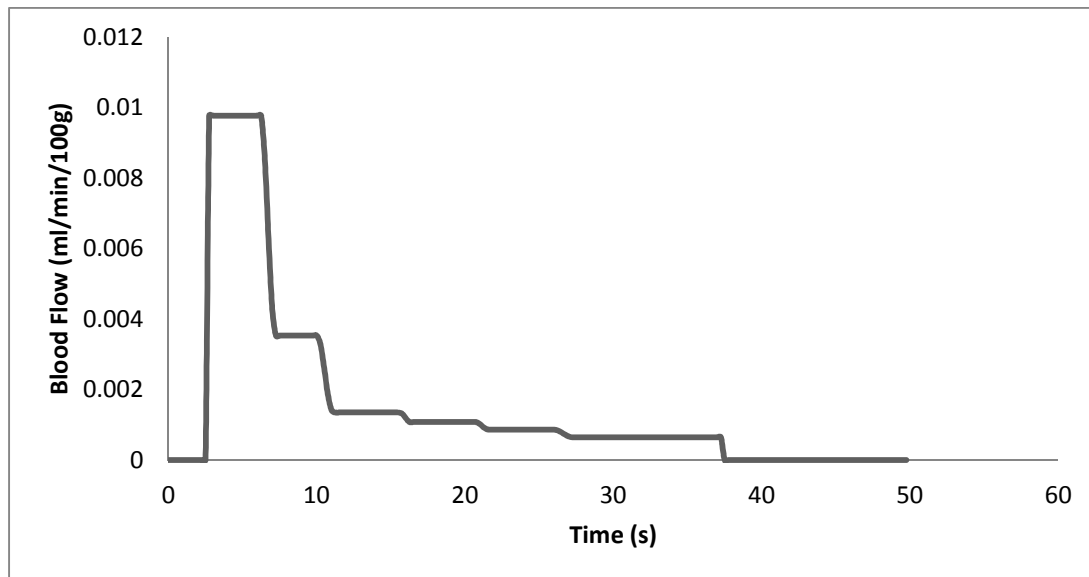
Where $*$ is the convolution operator, $Q(t)$ and $C_a(t)$ are the amount of ICG in the brain and arterial blood, respectively (Figure 1.3), F represents cerebral blood flow and $R(t)$ is referred to as the impulse residue function (Figure 1.4). It represents the amount of ICG in the brain region at any time t following an idealized bolus injection of unit concentration. Equation (1.6) indicates that in order to measure F , the time-dependent arterial and brain concentration must both be measured. With this technique, $Q(t)$ is determined by 2nd derivative NIRS and $C_a(t)$ is measured non-invasively by dye densitometry [66]. A deconvolution algorithm can be applied to the time-concentration data to extract a flow-scaled $R(t)$. Cerebral blood flow is given by the initial height of the function, since by definition $R(t)$ is initially equal to one, and the area under the function is equal to CBV. The MTT can be determined by the central volume principle, i.e., $CBV = MTT \cdot CBF$ [67]. Because deconvolution is extremely sensitive to noise, all data were analyzed using a stable algorithm that was developed specifically for ICG experiments [66].

Figure 1.3– Sample Arterial and Tissue ICG concentration curves



Representative tissue and arterial ICG concentration curves measured with NIRS and the dye densitogram unit. The peak arterial concentration is approximately 20 times greater than that of tissue concentration since the cerebral blood volume is about 5% of the total brain volume.

Figure 1.4– Sample flow-scaled impulse residue function



CBF-scaled impulse residue function $[F \cdot R(t)]$. The height of initial plateau equals

CBF and the area under the curve is CBV.

1.8 Cerebral Metabolic Rate of Oxygen

The cerebral metabolic rate of oxygen can be determined using the Fick Principle [68]:

$$CMRO_2 = CBF \cdot ([O_2]_a - [O_2]_v) \quad (1.7)$$

where $[O_2]_a$ is the arterial oxygen concentration and $[O_2]_v$ is venous oxygen concentration, which can be determined using the NIRS measurements of tissue [HHb]. Since NIRS measures the total blood [HHb], this procedure requires assuming a relative distribution of blood in arterial, capillary and venous blood compartments: 20%, 10%, and 70% respectively [69]. The venous concentration of oxygen is determined by:

$$[Venous O_2] = \left\{ [Hb]_T - \left[\frac{4}{3} \frac{[Hb]_T}{CBV \times \rho} - \frac{1}{3} [Hb]_a \right] \right\} \times 1.39 ml \frac{O_2}{g} Hb \quad (1.8)$$

This method has been validated *in vivo* in newborn piglets by comparison to $CMRO_2$ derived from directly measuring the oxygenation of venous blood collected from the superior sagittal sinus. In one study [70], piglets were subject to five cerebral metabolic states created by different anesthetics. No significant differences were found between $CMRO_2$ measurements obtained from NIRS venous oxygen measurements and those obtained from sagittal-sinus blood samples at any anesthetic level. Across all metabolic conditions, a strong correlation between the two techniques was found ($R^2 = 0.88$). The same validation approach was used in a subsequent study to demonstrate the accuracy of the NIRS $CMRO_2$ measurements following HI [71].

1.9 Assessing the Effects of Hypoxia-Ischemia on Cerebral Energy

Metabolism by NIRS

There have been several studies that have used NIRS to assess the effects of HI on cerebral oxygenation and blood flow. Recently, Kurth *et al.* 2009 [72] investigated the relationship between HI duration and cerebral oxygen saturation (S_cO_2) to establish a viability threshold that predicts neurological outcome. A correlation between the duration of S_cO_2 below 35% and neurological outcome was reported, suggesting that this NIRS measure of injury duration could be used to predict neurological outcome. In contrast, Ioroi *et al.* 2002 [73] demonstrated in newborn piglets that S_cO_2 quickly recovered to baseline values during reperfusion, despite evidence of reduced brain activity measured by aEEG. The inability to detect post-HI alternations in brain activity suggests that a more sensitive NIRS marker of cerebral energy metabolism is required. One approach is to use NIRS to measure $CMRO_2$ using the technique outlined in section 1.8.

Tichauer *et al.* was the first to use NIRS to investigate potential post-insult changes in $CMRO_2$ [71, 74, 75]. In an animal model of neonatal HI, $CMRO_2$ was found to be suppressed after HI and remained significantly depressed compared to pre-HI values for 6 h. Interestingly, post-HI CBF and [HHb] values between controls and HI groups were not significantly different after 30 min of reperfusion, demonstrating the importance of measuring $CMRO_2$ directly. In a subsequent paper, post-HI suppression in cerebral metabolism was strongly correlated with the duration of HI at 12 h after the insult [74]. It was postulated that the delay in the correlation

between insult duration and cerebral metabolism could be attributed to the effects of anesthesia. In a subsequent study, experiments were repeated using a lighter anesthetic (fentanyl) and it was shown that the correlation between $CMRO_2$ and HI was observable 45 min after the insult [75]. It was also demonstrated that a linear relationship between the mean voltage measured by amplitude-integrated EEG and $CMRO_2$ existed. This latter result brings up an important question regarding the mechanisms controlling cerebral energy metabolism following HI: Do the changes in $CMRO_2$ reflect mitochondrial dysfunction, as discussed above in Section 1.3.2, or do they reflect a reduction in energy demand due to reduced electrocortical activity, as suggested by the correlation with EEG [75]?

Understanding the possible mechanisms controlling cerebral energy metabolism during the reperfusion phase would help assess the value of $CMRO_2$ as a clinical marker of HI. That is, if metabolic depression observed by NIRS indicates mitochondrial impairment then it could be used as an early marker of secondary brain injury. As discussed in Section 1.3.2, the potent effects of NO on mitochondrial energy production could be involved in the observed $CMRO_2$ suppression post HI [76]. Not only does elevated NO help to ‘kick start’ the processes leading to delayed brain injury, it has the immediate effect of inhibiting mitochondrial respiration [20]. Administration of NO inhibitors after HI has been shown to reduce brain injury and improve energy metabolism [77, 78]. To test whether impaired mitochondrial energy production is related to suppressed energy metabolism post HI, Winter *et al.* examined the relationship between $CMRO_2$ and the high-energy metabolites,

measured by magnetic resonance spectroscopy. A general recovery of the metabolites despite reduced $CMRO_2$ was observed during the early recovery period, suggesting sufficient energy production [79].

Another possible mechanism responsible for decreased $CMRO_2$ following HI is the increase in extra-cellular adenosine concentration. Adenosine A_1 receptors in the brain are known to greatly influence cerebral synaptic activity by mediating cell membrane polarization and controlling neuronal firing. During HI, the breakdown of ATP results in increased concentrations of adenosine and ADP. The accumulation of extra-cellular adenosine in the brain is known to lead to hyper-polarization of cells, greatly reducing synaptic activity and therefore depressing the brain's energy demands [80]. This may explain the similar reductions in magnitude of post-HI $CMRO_2$. Recently, an adenosine receptor antagonist was shown to abolish the metabolic depression during hypoxia in fetal sheep [80]. However, the role of adenosine following neonatal HI is unclear since adenosine antagonists were shown to have little effect on the extent of brain injury in neonatal rats [81]. The lack of an effect in these experiments may have been due to the severity of the hypoxic-ischemic insult. Clearly, there is a need to better understand the mechanisms controlling post-HI oxidative metabolism and how they relate to delayed brain injury considering that changes in $CMRO_2$ are one of the earliest measurable events following HI. Understanding these adenosine-mediated mechanisms is the focus of the experiments presented in chapter 3.

1.10 Clinical Applications of NIRS in CBF and $CMRO_2$

Measurements

An understanding of the rate of oxygen delivery and blood flow in sick infants undergoing intensive care is an important aim of neonatal diagnostic care. As NIRS is portable, safe and non-invasive, it is ideal for clinical studies. As early as 1988, one of the first NIRS studies measured CBF in newborns undergoing indomethacin treatment for asphyxiation [82]. A sizable reduction in CBF from 18 ml/min/100g to 7 ml/min/100g after treatment was observed due to the vaso-constrictive property of indomethacin. Bucher *et al.* validated NIRS CBF measurements by a comparison to measurements obtained with the ^{133}Xe clearance technique [51]. A similar comparison was conducted by Skov *et al.* [83] on newborns, showing that there was a strong correlation between the two techniques ($R^2 = 0.84$, $p < 0.0001$). Since these validation studies, there have been several studies using NIRS to assess CBF in newborns with neurologic injuries. Meek *et al.* [84] showed that CBF is significantly declined in preterm newborns suffering from intraventricular hemorrhages, while Bellinger *et al.* [85] observed that newborns showed increased brain perfusion while undergoing hypothermia treatment during cardiopulmonary bypass surgery. A good compilation of similar NIRS perfusion studies is given by Chakravarti *et al.* [86].

Yoxall *et al.* [87] was the first group to measure cerebral oxygen consumption (CMRO_2) in newborns using NIRS. They were able to show that oxygen metabolism is linearly related with increasing gestational age and their values were in a good agreement with values obtained in other more invasive studies. In a subsequent study, Kissack *et al.* showed that increased oxygen consumption during the first 3 days after

birth indicated increased cerebral activity as result of normal adaptation to extrauterine life [88]. Elwell *et al.* [89], reported a good agreement between their NIRS CMRO₂ measurements and previous values obtained with PET [90]. Recently, Roche *et al.*[91] followed 56 premature newborns of various gestational age and showed that relative CBF and CMRO₂ correlate better with postnatal age (R= 0.37 and 0.43, respectively) compared to SO₂ (R= -0.07). They concluded that, in the premature newborns, relative CBF and CMRO₂ measurements are more accurate biomarkers of the brain development than SO₂. In a follow-up study they demonstrated that NIRS could be used to measure regional developmental changes in CBF and CMRO₂ in newborns [92], similar to earlier studies using PET [93] and single-photon emission computed tomography (SPECT) [94].

The majority of these clinical NIRS studies use the HbO₂ flow tracer method to measure CBF, rather than an endogenous dye such as ICG. As mentioned earlier, this method suffers from poor repeatability and low precision compared to the ICG bolus-tracking approach. The appendix of this thesis will discuss a study using the NIRS/ICG technique to measure CBF in preterm newborns undergoing drug therapy for a common heart condition, patent ductus arteriosus.

1.11 Research Objective

- I. To provide a clearer understanding of the relationship between early changes in CMRO₂ and brain injury, the goal of the present study was to investigate a

potential mechanism underlying the observed reductions in $CMRO_2$ following HI. Elevated adenosine levels, as observed during HI, are known to inhibit synaptic activity and reduce metabolic demand via adenosine A_1 receptor. Studies have shown that blocking these adenosine receptors during hypoxia (ischemia) with a specific adenosine A_1 receptor antagonist, 8-cyclopentyl-1,3-dipropylxanthine (DPCPX), diminished the cerebral metabolic depression during hypoxia. The objective of this study was to investigate if the same adenosine A_1 receptor antagonist affects the $CMRO_2$ and synaptic activity (aEEG) depression following HI in neonatal piglets.

CHAPTER 2 - METHODS & MATERIALS

2.1 Animal Preparation

The study was approved by the Animal Use Subcommittee of the Canadian Council on Animal Care at the University of Western Ontario. Newborn Duroc piglets were delivered from a local supplier on the morning of the experiment. All surgical procedures were performed under 3% isoflurane. Piglets were tracheotomized and mechanically ventilated on a 2:1 oxygen/medical-air mixture. Two incisions were made lateral to the trachea, and vascular occluders (In Vivo Metric, Healdsburg, CA) were placed around both carotid arteries just proximal to the carotid bifurcation. A cannula was inserted into an ear vein for injecting the NIRS contrast agent (indocyanine green, ICG) and another cannula was inserted into a belly vein for infusing 8-cyclopentyl-1,3-dipropylxanthine (DPCPX) and fentanyl. A final cannula was inserted into a femoral artery for continuous monitoring of blood pressure and to allow the collection of arterial blood samples for gas and glucose analysis. Following surgery, isoflurane was reduced to 1.75%, and piglets were allowed to stabilize for 1h before the experiment started.

2.2 Experimental Procedure

Piglets were randomly divided into two groups: a drug group (i.e. those who received DPCPX) and a control group (i.e., those who received the vehicle). For the baseline NIRS measurements of CBF and CMRO₂, the anesthetic was switched from isoflurane to a combination of an i.v. infusion of 0.02 mg/kg/h fentanyl and the inhalation of 30% oxygen/70% N₂O gas mixture. Two measurements were acquired,

separated by 10 min to allow time for the concentration of ICG in the blood to equilibrate. The anesthetic was switched to fentanyl/nitrous oxide because this combination has less of an effect on cerebral metabolism than isoflurane [95]. Following the baseline measurements, isoflurane anesthesia was reinstated for the hypoxic-ischemic insult to replicate the HI protocol used in our previous studies [71, 74, 75]. After a period of 45 min, a hypoxic-ischemic insult was induced by clamping both carotid arteries and reducing the fraction of inspired oxygen to 7%. Based on a threshold established in our previous study, ischemia was defined when the mean arterial pressure (MAP) fell to less than 70% of baseline [74]. All piglets were then subjected to 10 min of ischemia, after which the carotid clamps were released and the fraction of inspired oxygen returned to baseline levels.

For the drug group, DPCPX was infused intravenously for 30 min prior to the start of HI, discontinued during HI, and then continued again for another 30 min after the insult had ended. DPCPX infusion was paused during HI as a precaution because this drug is known to elevate heart rate, which can lead to cardiac arrest during stressful conditions [96]. DPCPX was prepared in 0.1M NaOH to a concentration of 2.5mg/min with a final pH of approximately 10. The drug was infused at a rate of 2.5 mg/min for the first 10 min and at 0.75 mg/min for the remainder of the infusion period [80]. The same infusion protocol was followed for the control group using only the vehicle (no DPCPX). After the hypoxic-ischemic insult, the anesthetic was again switched from isoflurane to the fentanyl/N₂O mixture. After 30 min of reperfusion, four NIRS measurements of CBF and CMRO₂ were collected with each

measurement separated by at least 10 min to allow time for ICG clearance. EEG data were collected continuously throughout the study.

At all times during the experiment (excluding the insult), arterial PCO_2 was maintained between 38–42 Torr by adjusting the respiratory rate, and arterial PO_2 was maintained between 100–150 Torr by adjusting the ratio of oxygen to medical air. Blood glucose was kept between 3 and 8 mmol/l by intermittent 0.3-ml injections of a 25% dextrose solution into an ear vein. A water-heating blanket was used to maintain a rectal temperature between 37 and 38°C. Arterial pH and heart rate were also monitored.

2.3 Near-Infrared Spectroscopy

NIRS data were collected with a continuous-wave, broadband (600 –1,000 nm) system with a single emission fiber-optic bundle and a single detection bundle [66]. The end of each bundle was placed 3 cm apart, parasagittally on the head, proximal to the widest part of the brain. The bolus-tracking technique for measuring CBF involved measuring the time-dependent concentration of ICG in arterial blood and brain tissue following a rapid intravenous injection of the dye (0.1 mg/kg). The arterial blood ICG concentration curve was measured by a dye densitometer attached to a front paw and the brain ICG concentration curve by NIRS. Both concentration curves were acquired over a period of approximately 60 s, and a deconvolution was applied to the data to extract estimates of CBF, cerebral blood volume (CBV) [66] and subsequently CMRO_2 . The exact methods used to calculate CBF and CMRO_2 by

NIRS have been outlined in detail previously [66, 68, 70] and briefly in the introduction (Chapter 1 Sections 1.7 and 1.8).

2.4 Electroencephalography

To assess electrocortical brain activity, needle electrodes were inserted to record from the left and right parietal regions of the brain. The signal was recorded at a sampling rate of 250 Hz after being amplified and filtered (0.1–100 Hz) using a high-performance AC preamplifier (model P511, Grass Technologies Product Group, Astro-Med, West Warwick, RI). An algorithm developed in MATLAB (The MathWorks, Natick, MA) was used to convert the raw EEG data to an aEEG signal [75]. Data were filtered, rectified, and integrated over a window of 100 ms. To eliminate non-physiological signal components and to attenuate the dominant delta-wave patterns, a series of filters were applied to mimic those used in the Cerebral Function Monitor [97]. The final signal was plotted logarithmically, and the resulting aEEG was analyzed by two different methods: a quantitative mean aEEG background technique and a qualitative neural activity score technique.

The mean aEEG background signal was measured by drawing a line through the upper and lower margins of the aEEG band, as described by al Naqeeb *et al.* [37]. In this way, individual spikes separated from the aEEG band are excluded from the measurement. The median line between the upper and lower margins was taken to be the mean amplitude. A neural activity score, reflecting the functional state of the brain, was calculated based on the background voltage and pattern recognition. Specifically, the background voltage was graded as normal, low, or extremely low.

The background pattern was classified as either continuous or discontinuous, and the presence of seizure activity or burst-suppression pattern was noted [98]. The aEEG data from each experiment were scored in 10-min intervals and then grouped to calculate a mean neural activity scores for baseline and reperfusion periods.

2.5 Statistical Analysis

SPSS 17.0 (SPSS, Chicago, IL) was used for all statistical analyses. A two-way, mixed analysis of variance (ANOVA) with Bonferroni post-hoc correction was used to compare measurements between drug and vehicle/control groups, with time as the within-subjects variable and treatment as the between-subjects variable. The analysis was conducted for average pre- and post-HI values of CBF, OEF, CMRO₂ and EEG. When appropriate, group differences at individual time periods were investigated by a Student's t-test. For nonparametric data, such as the neural activity scores, the Spearman's rank test was used. Statistical significance for all tests was based on a $P < 0.05$. All values are presented as means \pm SE.

CHAPTER 3 - RESULTS

A total of 20 piglets (9 males, 11 females) were studied. Three females in the drug group could not be revived during HI due to cardiac complications and were therefore excluded from the results. There were a total of 10 piglets in the drug group and 7 in the control group (average age: 27 ± 5 h, weight: 1.58 ± 0.06 kg). Table 3.1 summarizes the results of the physiological parameters for each group at baseline and during reperfusion. No significant differences were found between the two groups for any of these parameters. Although both groups showed a trend of increased heart rate after HI, this effect did not reach significance. All other physiological parameters remained within their normal range.

The duration of ischemia, as defined by MAP below 70% of baseline, was not significantly different between the two groups: 10 ± 1.58 min for the vehicle group and 10.92 ± 1.48 min for the drug group. However, the total duration of carotid clamping and reduced inspired oxygen was significantly longer for the drug group (25.3 ± 1.45 min) compared to the vehicle group (14.4 ± 1.86 min). This difference suggests that DPCPX delayed the onset of loss of autoregulation caused by HI.

Figure 3.1 presents average CBF, OEF and $CMRO_2$ values for the drug and vehicle groups at baseline and during reperfusion. Significant time ($p < 0.001$) and treatment effects ($p < 0.001$) were found for CBF, but no overall time-by-treatment interaction was observed. Average baseline CBF values for the vehicle and drug groups were 50.86 ± 3.59 and 60.58 ± 5.67 ml/min/100g, respectively, which were not significantly different. In both groups, CBF fell by roughly 20% following HI to

40.55 and 48.5 ml/min/100g for the vehicle and drug group, respectively. Figure 3.1B presents the average OEF values for the two groups pre- and post-HI. No significant time or treatment effect was found, nor was there a significant time-by-treatment interaction.

Figure 3.1C presents the average CMRO₂ values for the drug and vehicle groups at baseline and after reperfusion. A significant time-by-treatment interaction was found ($F(3,66) = 4.81, p < 0.05, \text{power} = 0.68$) with a significant overall time effect ($p < 0.001$). The source of the interaction was the difference in the post-HI CMRO₂ values ($p < 0.05$), whereas, there was no significant difference between groups at baseline. Average baseline values were 2.71 ± 0.06 and 2.52 ± 0.12 ml O₂/min/100g for the vehicle and drug groups, respectively. A significant decrease in CMRO₂ was observed for the vehicle group compare to baseline, with an average post-HI value of 1.88 ± 0.18 ml O₂/min/100g ($p < 0.001$). For the drug group, CMRO₂ decreased to 2.25 ± 0.21 ml O₂/min/100g after HI, but this change was not significant from its baseline value.

Figure 3.2A presents the average aEEG values for both groups at baseline and during reperfusion. There were overall significant time ($p < 0.01$) and treatment ($p < 0.01$) effects, as well as a significant time-by-treatment interaction ($F(3,66) = 3.9, p < 0.05, \text{power} = 0.70$). There was no significant difference in baseline aEEG measurements between the two groups with average values of 48.5 ± 1.6 and 50 ± 1.52 μV for the vehicle and drug group, respectively. Post-hoc analysis revealed a significant difference between the two groups following HI ($p < 0.01$). For both

groups, aEEG dropped significantly after HI: $34 \pm 5.6 \mu\text{V}$ for the drug group ($p < 0.01$) and 21.8 ± 4.8 ($p < 0.001$) for the vehicle group. A significant difference in the time between the start of HI and the resulting reduction in aEEG activity was also observed (Figure 3.3). This delay was significantly shorter for the vehicle group (3.67 ± 1.03 min) compared to the drug group (15.2 ± 3.97 min).

Figure 3.2B presents the averaged neural score values for the two groups before and after HI. Significant time ($p < 0.001$) and treatment ($p < 0.001$) effects and a significant time-by-treatment interaction were observed ($F(3,66) = 39.7$, $p < 0.001$, power = 0.86). For piglets in the drug group, the average neural score dropped to 3.3 ± 0.4 during the reperfusion period. However, this difference was not significant compared to baseline. The neural score for the vehicle group dropped significantly to 2.1 ± 0.4 ($p < 0.001$) during the reperfusion period. An inter-group comparison showed there was a significant difference in neural scores between the post HI periods of the 2 groups ($p < 0.001$).

Table 3.1 Physiological variables for the drug and vehicle groups before insult (baseline) and during reperfusion.

	Baseline	Post Insult
Mean Arterial Pressure (Torr)		
Vehicle	70.4 ± 1.53	67.67 ± 2.29
Drug	65.54 ± 2.46	67.07 ± 2.03
Heart Rate (beats/min)		
Vehicle	197.25 ± 7.47	206 ± 5.82
Drug	171.84 ± 10.16	201.24 ± 12.7
Arterial pCO₂ (Torr)		
Vehicle	40.18 ± 1.08	39.69 ± 0.66
Drug	39.72 ± 0.87	39.53 ± 0.69
Arterial pO₂ (Torr)		
Vehicle	123.13 ± 5.23	128.25 ± 2.68
Drug	123.36 ± 2.84	122.7 ± 2.63
Arterial pH		
Vehicle	7.37 ± 0.05	7.35 ± 0.03
Drug	7.40 ± 0.04	7.41 ± 0.03

Values are mean ±SE

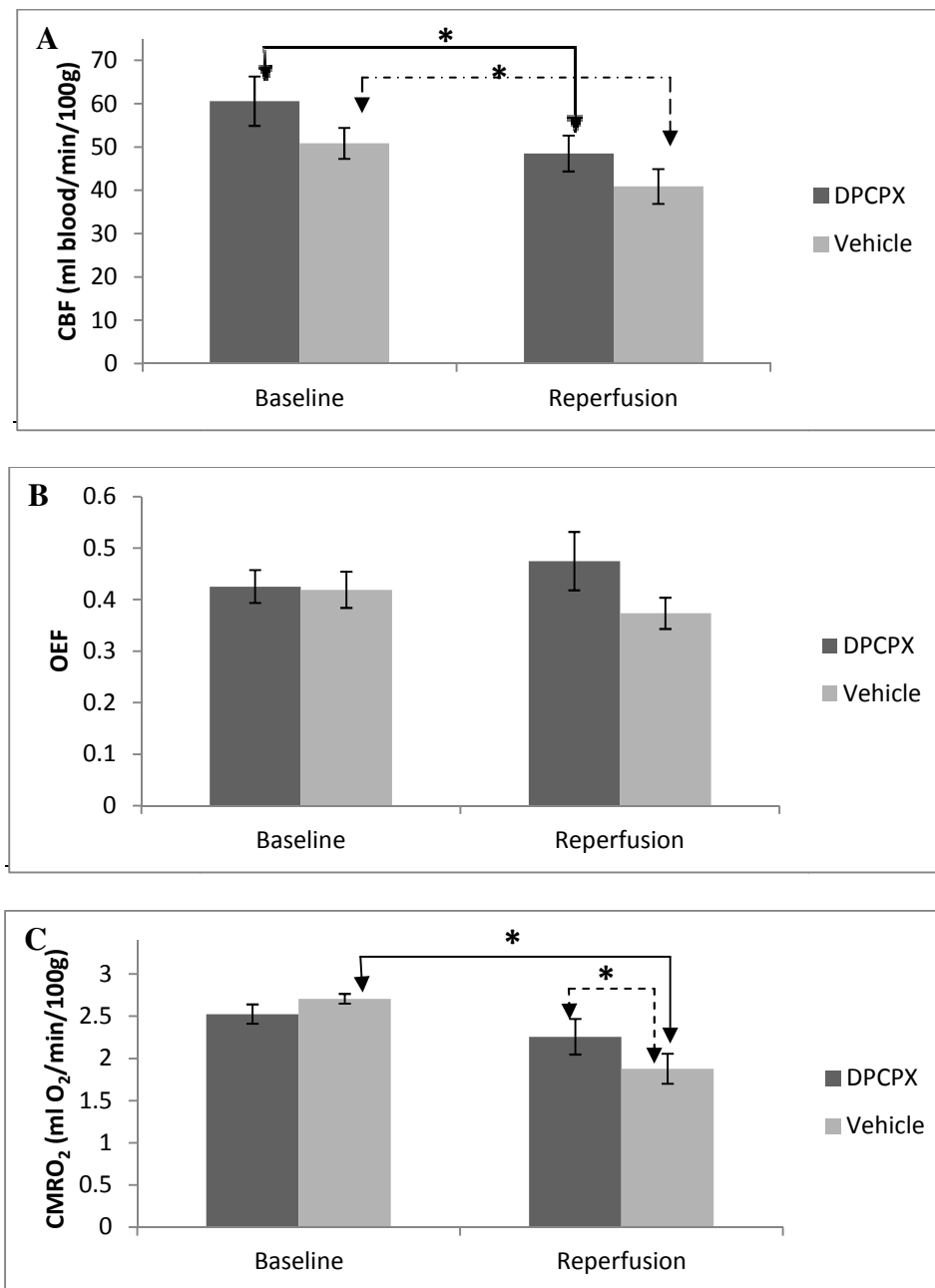


Figure 3.1 Comparison of (A) cerebral blood flow (CBF), (B) oxygen extraction fraction (OEF) and (C) cerebral metabolic rate of oxygen (CMRO₂) between treatment (DPCPX) and vehicle groups at baseline and after HI. Error bars represent SE and * indicates statistical significance.

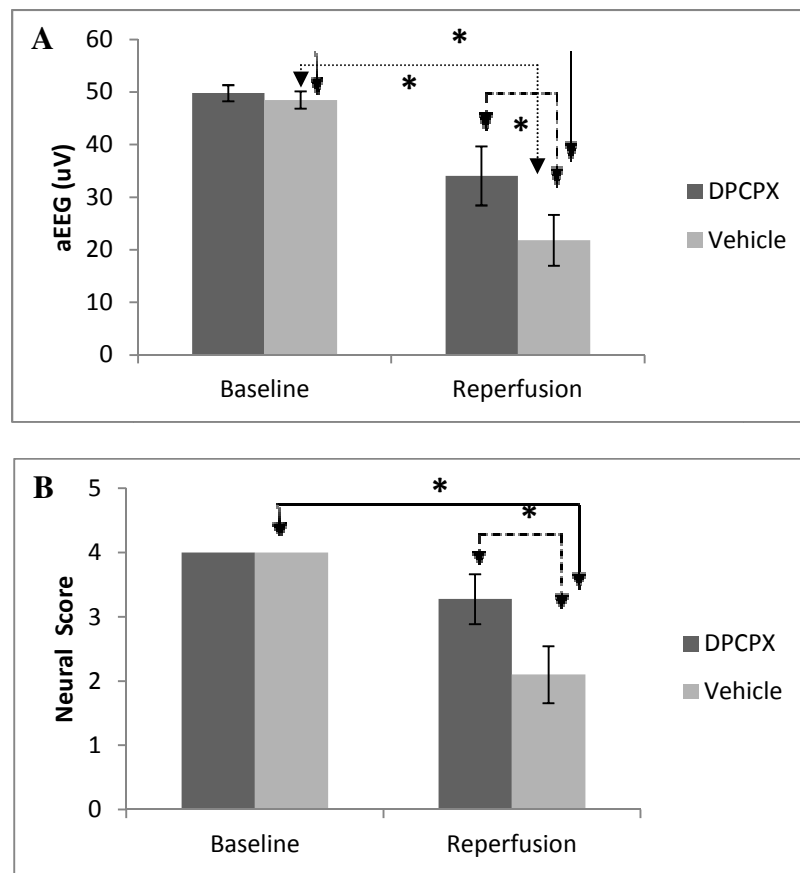


Figure 3.2 Comparison of (A) mean amplitude-integrated electroencephalography (aEEG) and (B) neural scores between treatment (DPCPX) and vehicle groups at baseline and post HI. Error bars represent SE and * indicates statistical significance ($p < 0.05$).

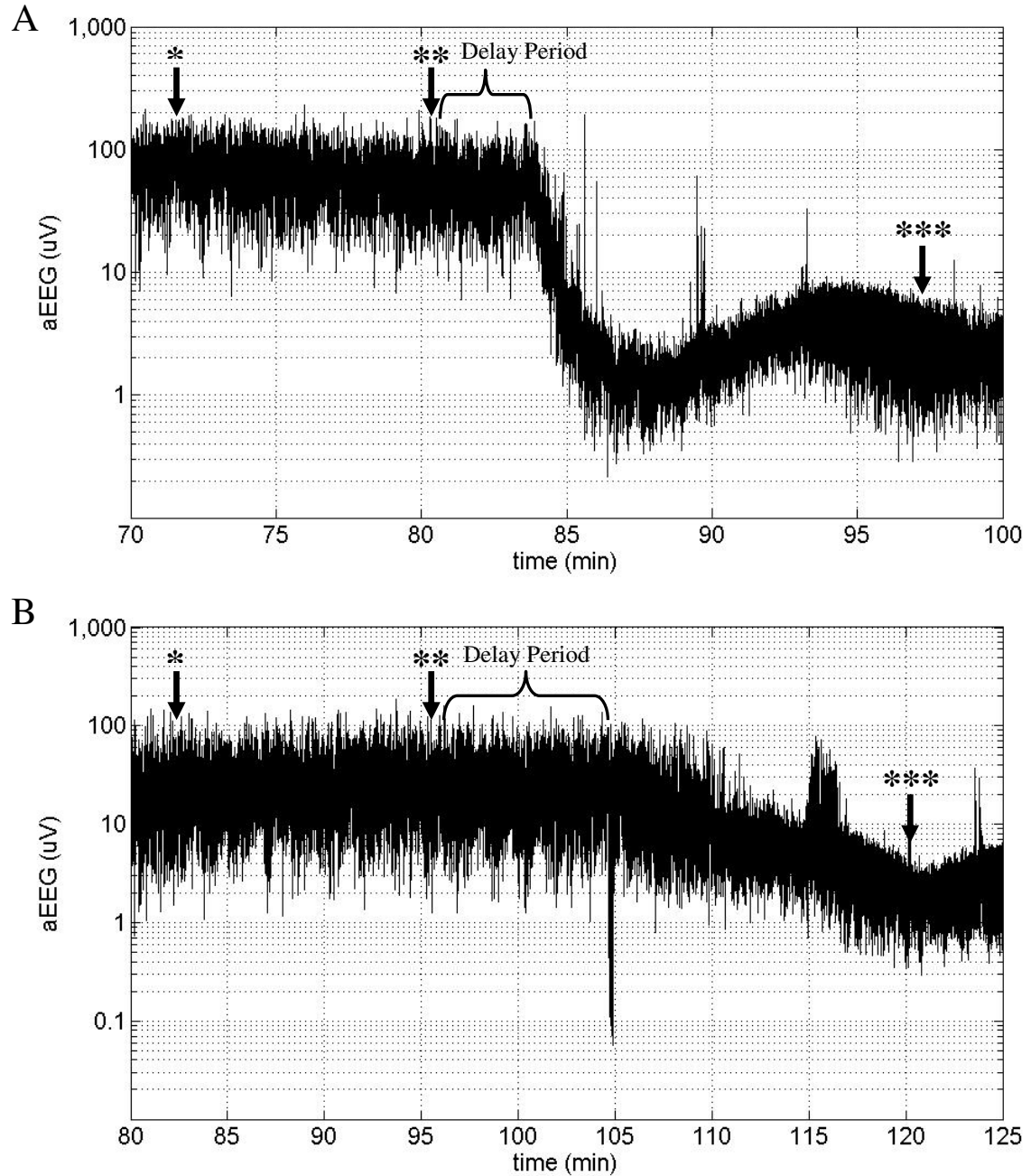


Figure 3.3 Continuous amplitude-integrated electroencephalography (aEEG) recording plotted against time for one animal in the treatment (DPCPX) group (A) and another animal in the vehicle (B). *indicates start of drug/vehicle infusion, ** indicates start of insult conditions and *** indicates the end of insult.

CHAPTER 4 - DISCUSSION

The brevity of the therapeutic window highlights the need to quickly identify infants at risk of HIE in order to maximize treatment efficacy [99]. One approach is to measure cerebral energy metabolism since impaired metabolism has been suggested as an early marker of delayed brain injury [16]. Our group and others have previously shown in an animal model of HI that $CMRO_2$ is depressed following an hypoxic-ischemic insult; however, the mechanisms controlling post-HI $CMRO_2$ were unclear [71, 74, 77, 78]. The principle finding of the current study was that the administration of the adenosine A_1 receptor antagonist, DPCPX, significantly reduced the metabolic depression following moderate HI. Considering that adenosine concentrations are known to rise during HI and have been shown to substantially suppress electrocortical synaptic activity [100-102], these results suggest that the observed post-HI reduction in $CMRO_2$ was most likely due to reduced cerebral energy demands. This conclusion was substantiated by the results from the concurrent aEEG recordings, which displayed significantly less electrocortical suppression after HI in animals administered DPCPX.

The role of adenosine in suppressing electrocortical activity and cerebral energy metabolism under conditions that lead to oxygen deprivation has been demonstrated in a number of studies. Administering DPCPX in near-term fetal sheep undergoing 10 min of umbilical cord occlusion was shown to delay the rapid decline in EEG intensity that was observed at the beginning of cord occlusion in control animals [103]. Similarly, the time to electrocortical suppression following global

cerebral ischemia was significantly longer in rats administered DPCPX [104]. This specific adenosine A₁ receptor antagonist has also been shown to increase the recovery rate of spontaneous electrocortical activity following transient global ischemia [105]. Regarding cerebral energy metabolism, Blood *et al.* showed that DPCPX completely abolished the reduction in cortical heat production – an indicator of cortical metabolism [103] – that occurs during cerebral hypoxia [80]. DPCPX treatment was also found to attenuate the reduction in heat production during cord occlusion [106]. The results of the current study are in good agreement with these previous studies. In piglets treated with DPCPX, the suppression of EEG activity following the onset of HI was delayed by approximately 10 min compared to controls. Furthermore, post-HI CMRO₂ and mean aEEG voltage were significantly greater in treated animals, although the latter remained below pre-HI values in both groups. This general agreement suggests that activation of the adenosine A₁ receptor due to the rise in adenosine concentrations during HI is the primary reason for reduced CMRO₂ following an hypoxic-ischemic insult. It is generally considered that the adenosine-induced reduction in cerebral metabolism is a neuroprotective response [107, 108]. For instance, Halle *et al.* demonstrated that enhancing the binding of adenosine to its A₁ receptors resulted in substantially reduced brain injury following HI in newborn rats [109].

In contrast to the above findings, Jensen *et al.* reported that treatment with DPCPX had little to no effect on cerebral metabolism or EEG intensity in fetal sheep exposed to 10 min of asphyxia [110]. Compared to baseline values, significant

reductions in EEG intensity and cortical heat production were observed during the first 4 h after occlusion. One possible reason for the discrepancy between the two studies could be differences in the severity of asphyxia. The 10-min cord occlusion model was classified as a severe injury as demonstrated by significant neuronal loss [111]. In the current study, all piglets were subjected to 10 min of ischemia; however, the severity of ischemia is likely less than during complete cord occlusion due to residual blood flow through the vertebral arteries [71]. Furthermore, the correlation between the degree of neuronal damage, as indicated by the number of Fluoro-Jade B positive cells, and ischemia duration would indicate that a 10-min insult would likely be classified as a mild-to-moderate injury [74]. This explanation would also agree with the reported differences in the effects of DPCPX on cerebral metabolism during hypoxia [80], which showed attenuation of metabolism post-HI, compared to severe asphyxia [106] which did not. Another explanation could be the difference in the DPCPX infusion protocol used in the two studies. With the cord occlusion model, the DPCPX infusion was stopped at the end of the occlusion period, whereas, in the current study the infusion was continued for another 30 min. It may be that the infusion during the early post-HI period was necessary to abolish the effects of residual adenosine from the hypoxic-ischemic period.

The results of the current study also complement the findings of our previous study that combined NIRS measurements of $CMRO_2$ with phosphorous (^{31}P) and proton (1H) magnetic resonance spectroscopy [79]. In that study, a general recovery of high-energy metabolites and a reduction in lactate concentration in the brain were

found during the recovery period following 30 min of HI, despite depressed CMRO₂. It was postulated that the discrepancy between CMRO₂ and metabolite levels reflected a reduction in cerebral energy demands following HI rather than impaired energy production. Similar results were found in the current study as evident by the concurrent reductions in post-HI aEEG intensity and CMRO₂ in the control animals. Furthermore, the increase in both of these measures in the DPCPX-treated animals suggests a possible mechanism to explain these findings.

Another potential mechanism contributing to the metabolic changes observed following HI is nitric oxide. Increased neuronal and inducible nitric oxide synthase (NOS) expression has been observed during the first 6 h following HI [18, 112], and it is known that elevated NO levels can reduce mitochondrial respiration by inhibiting cytochrome c oxidation. [20, 113]. Peeters-Scholte *et al.* demonstrated in newborn piglets that the use of selective (neuronal and inducible) NOS inhibitors, following 60 min of HI, reduced brain cell damage and improved the cerebral energy state, as characterized by the recovery of the concentration of high-energy metabolites (phosphocreatine and ATP) [77]. Dorrepaal *et al.* demonstrated in fetal lambs that infusing a non-selective NOS inhibitor after HI prevented the expected decrease in CMRO₂ and showed a delayed improvement in electrocortical brain activity [78]. One possible link between these studies and the current results is the involvement of the adenosine A₁ receptor in the up-regulation of nitric oxide synthesis and signaling [114, 115]. Using an *in-vitro* model of cerebral ischemia, Barth *et al.* demonstrated that activation of A₁ receptors increased nitric oxide production, which lead to

increased neuronal damage [116]. Although these results appear to conflict with the concept that adenosine is a neuroprotector, elevated NO production occurred at relatively high adenosine concentrations ($> 10 \mu\text{M}$). Further studies involving *in-vivo* models could help to better elucidate the potential relationship between adenosine, nitric oxide synthesis, and cerebral metabolism. One approach would be to measure markers of elevated NO production in animals treated with DPCPX [76].

In the current study, both the DPCPX group and controls showed a significant CBF reduction of approximately 20% after HI. Cerebral hypoperfusion has been reported previously with other animal models of hypoxia-ischemia [117, 118]. The concurrent reduction in both CBF and CMRO_2 in the control group suggests that the post-HI hypoperfusion is a result of the coupling between CBF and cerebral energy metabolism. However, there was no increase in CBF in the DPCPX group despite the significant increase in post-HI CMRO_2 . Instead, a trend of elevated OEF was observed, although it did not reach statistical significance. It is difficult to interpret the CBF results, as we have observed considerable variability in post-HI perfusion changes in previous studies with both significant hypoperfusion and full recovery reported [71, 74]. Unlike CMRO_2 , a significant correlation between CBF and insult duration was not observed [75].

CHAPTER 5 - SUMMARY

5.1 Summary

The cascade of events leading to the depression of cerebral oxidative metabolism after hypoxia-ischemia is complex [7]. The present study demonstrates that blocking the adenosine A₁ receptor significantly diminished the depression of CMRO₂ and aEEG typically observed following HI. These results suggest that post-HI cerebral energy metabolism is at least, in part, controlled by an adenosine-mediated mechanism. These results complement earlier studies showing similar effects in the fetal brain during hypoxia. However, more studies are required to determine if this mechanism has a role following more severe hypoxia-ischemia and if these changes are ultimately related to the final extent of brain injury.

5.2 Limitations

5.2.1 Limitations of the Near-Infrared Spectroscopy Cerebral Metabolic Rate of Oxygen Measurement

There are three primary limitations to the NIRS method described for measuring CMRO₂. The most important is the assumption that the relative arterial and venous fractions of the cerebral blood volume are known. NIRS measurements cannot distinguish between the arterial, capillary, and venous compartments of the cerebral circulation and thus reflect a weighted average of Hb concentrations within these different blood compartments in the region sampled. The relative distribution of arterial, capillary, and venous compartments in the CBV is generally accepted to be approximately 20%, 10%, and 70% respectively [69]. Assuming that the capillary

concentration of HHb is the average of arterial and venous concentrations, the final CBV distribution would equate to 25% arterial blood and 75% venous blood. There is some acceptable variability (10%) in the ratio from individual to individual [119]. The second assumption is that the cerebral water concentration is known (85%), which is used to calculate the differential pathlength of light. The water content of the brain is known to be very stable, and has been shown to only increase by less than one percent 24 h after hypoxia-ischemia in neonatal rats [120]. The final potential limitation is the use of an exogenous contrast agent to measure CBF. The advantage of using indocyanine green (ICG) is increased measurement precision compared to CBF measurements obtained with the HbO₂ tracer method [63]. However, ICG, like all contrast agents, has the risk of causing allergic reactions, albeit fairly small [56, 57]. Therefore, the clinical use of this technique requires a careful consideration of the risks versus the potential benefit.

5.2.2 Limitations of Assessing the Effectiveness of DPCPX

This study lacked independent measurements of the cerebral adenosine concentration to verify an increase after HI. However, elevated adenosine concentrations within the brain have been previously demonstrated in rats during hypoxia [100], as well as in the blood plasma in patients during ischemia [121]. Another potential limitation is that the study did not include any measure of neuronal damage, such as by Fluro-Jade staining [74, 122], to determine if the changes in CMRO₂ caused by DPCPX treatment would exacerbate brain injury. However, this

effect has been previously demonstrated [106]. Furthermore, the objective of this study was to investigate the mechanisms controlling changes in cerebral energy metabolism immediately following HI since an earlier study demonstrated a correlation between early $CMRO_2$ changes and the severity of HI [74]. This correlation suggests that measuring $CMRO_2$ by NIRS could help to identify newborns at risk of developing HIE.

5.3 Future Work

5.3.1 Investigate Alternate Mechanisms Controlling $CMRO_2$ Post-HI

As mentioned in the Discussion, there appears to be two competing mechanisms that control $CMRO_2$ after HI: adenosine and nitric oxide. It has been suggested that these two mechanisms interact as elevated adenosine levels could increase NOS [116], while other studies suggest that they act independently [123]. Due to the lack of *in vivo* evidence, however, how or if adenosine and nitric oxide interaction remains to be verified. This is of potential interest for future work using the current model of HI in piglets with the adenosine antagonist (DPCPX) and the incorporation of a neuronal and inducible nitric oxide (synthase) inhibitor.

5.3.2 Clinical Implementation of NIRS

The NIRS measurements of $CMRO_2$ were shown to be sensitive to a hypoxic-ischemic injury within the first couple of hours after reperfusion. Furthermore, NIRS could be used as a safe, portable, complementary diagnostic tool to accurately predict

the extent of brain injury incurred by hypoxia-ischemia and other neonatal brain disorders. For example, the technique may have implications in the diagnosis of both intraventricular hemorrhage and periventricular leukomalacia, which are common forms of brain injury in preterm neonates, and each with hemodynamic and metabolic sequelae [33]. Lastly, this technique has the potential to substantially benefit the monitoring and care of critically ill and very low birth weight infants requiring medical intervention. The appendix of this thesis refers to one recently completed pilot study that successfully used this NIRS technique to assess cerebral perfusion and metabolic changes in preterm newborns.

5.4 Conclusions

The most significant findings of the thesis are:

1. Post-HI cerebral energy metabolism is in part controlled by an adenosine-mediated mechanism. Blocking the adenosine A_1 receptor significantly diminished the depression of $CMRO_2$ and aEEG typically observed following HI. This suppression of cerebral metabolism and electrocortical activity following HI is most likely a neuroprotective response.
2. Both NIRS and EEG techniques can be applied simultaneously at the bedside of sick newborns, which could help to improve the diagnosis of hypoxic-ischemic encephalopathy by providing early detection of those infants that would benefit from therapy.

APPENDIX A

The contents of this chapter have been adapted from the paper entitled “*A near-infrared spectroscopy study to assess the effects of Indomethacin on cerebral blood flow and metabolic rate of oxygen in preterm infants*”, in the process of publication in the *Journal of Pediatric Research* by Arora R, Ridha M, *et al.*

Responsibilities: Acquisition and analysis of the majority of the data.

Introduction

The ductus arteriosus is a vascular structure within the heart that connects the aorta to the pulmonary artery. This fetal structure normally closes spontaneously after birth. However, in cases where the ductus remains open, known as patent ductus arteriosus (PDA), it poses a greater risk for pulmonary edema, hemorrhage and decreased perfusion and oxygen delivery to the organs, including the brain [124]. The incidence of PDA is inversely correlated to birth weight and gestational age, with approximately 40% of infants having a PDA who are below 1000 g or of a gestational age less than 28 weeks [125, 126].

Treatment of PDA is commonly in the form of a non-steroidal anti-inflammatory drug (NSAID). Two primarily used ones clinically are: indomethacin and ibuprofen [127, 128]. These drugs act similarly by inhibiting the production of prostaglandins, constricting the ductus arteriosus, which induces anatomical remodeling and ultimately ductal closure. Both drugs have the same efficacies with success rates ranging between 60 to 80% [129]. The only notable difference between

the two drugs is the physiological side-effect of indomethacin as a vasoconstrictor, which has been shown to reduce renal and cerebral perfusion. The latter effect is of particular interest considering this is a patient population that is already at high risk of brain injury. Thus alterations in cerebral hemodynamics as a consequence of PDA treatment remains a concern [128], particularly if these reductions are large enough to affect cerebral energy metabolism.

The objective of the present study was to measure cerebral blood flow (CBF), oxygen extraction fraction (OEF) and cerebral metabolic rate of oxygen ($CMRO_2$) in preterm infants with a hemodynamically significant PDA who have been selected to receive treatment with indomethacin. Measurements were obtained prior to and immediately following the infusion of the first dose of the drug, which was part of a standard three-dose (one dose per day) protocol. CBF was measured with the same bolus-tracking NIRS technique using the light-absorbing dye indocyanine green (ICG) as described in chapter 1 and 2.

Method

Preterm infants (GA < 30 weeks) with hemodynamically significant PDA (diagnosed based on clinical indices) were enrolled in the study after obtaining informed and written parental consent. All NIRS data were collected with a continuous-wave, broadband (600-980 nm) system using two fiber-optic bundles, one for light emission and the other for detection [66]. The ends of the fiber bundles were held 3.5 cm apart using a custom-built holder that was strapped to the infant's head to position the probes over the frontoparietal region. Measurements of $CMRO_2$, CBF

and OEF were determined using the same second derivative spectroscopy technique [130] described in Chapter 1 (Sections 1.7 and 1.8).

Pharmacological treatment of PDA followed the standard indomethacin dosage schedule consisting of three doses of 0.2mg/kg, each separated by 24 hours, infused intravenously over 30 min. Two NIRS data sets were acquired on the first day of treatment, one approximately 5 min prior to the start of drug infusion and the other immediately at the end of 30 min infusion. The acquisition period for each ICG run was approximately 80 s. The tissue and arterial ICG concentration curves were acquired simultaneously by NIRS and the DDG, respectively.

Results

Complete data sets (i.e., both NIRS and DDG data before and after first treatment dose) were obtained from 8 infants. Figure 1 shows the individual pre- and post-treatment values of CBF, CBV, OEF, and $CMRO_2$. A general reduction in CBF and CBV was observed as expected due to the known vasoconstricting effects of indomethacin. A concurrent increase in OEF was found while $CMRO_2$ displayed no significant change. These observations were confirmed by the mean pre- and post-treatment values given in Table 1. Indomethacin caused a significant decrease in CBF of 18% ($p < 0.025$) and in CBV of 17% ($p < 0.02$). There was a significant increase in OEF of 29% ($p < 0.025$), but the drug has no overall effect on $CMRO_2$. The PDA was closed in all eight cases after the three-dose regimen of indomethacin.

Table 1: Clinical parameters and near-infrared spectroscopy measurements before and after indomethacin infusion

Parameter	Pre	Post
MAP (mm Hg)	36.9 ± 2.7	38.7 ± 2.8
EtCO ₂ (mm Hg)	56.1 ± 2.4	56.0 ± 2.2
pH	7.28 ± 0.02	7.25 ± 0.01
Heart Rate (beats/min)	152 ± 4	156 ± 3
SaO ₂ (%)	93.6 ± 1.9	93.0 ± 2.0
CBF (ml·100g ⁻¹ ·min ⁻¹)	12.9 ± 1.3	10.6 ± 0.9*
CBV (mL·100 g ⁻¹)	2.05 ± 0.12	1.69 ± 0.09*
OEF	0.28 ± 0.03	0.36 ± 0.03*
CMRO ₂ (ml O ₂ ·100 g ⁻¹ ·min ⁻¹)	0.59 ± 0.06	0.65 ± 0.07

Values are mean ± SE (n = 8). MAP: mean arterial blood pressure, EtCO₂: end-tidal carbon dioxide tension, CBF, cerebral blood flow; CBV, cerebral blood volume; [HHb], tissue concentration of deoxy-hemoglobin; OEF, oxygen extraction fraction; CMRO₂, cerebral metabolic rate of oxygen

*Significant change with treatment (p < 0.05).

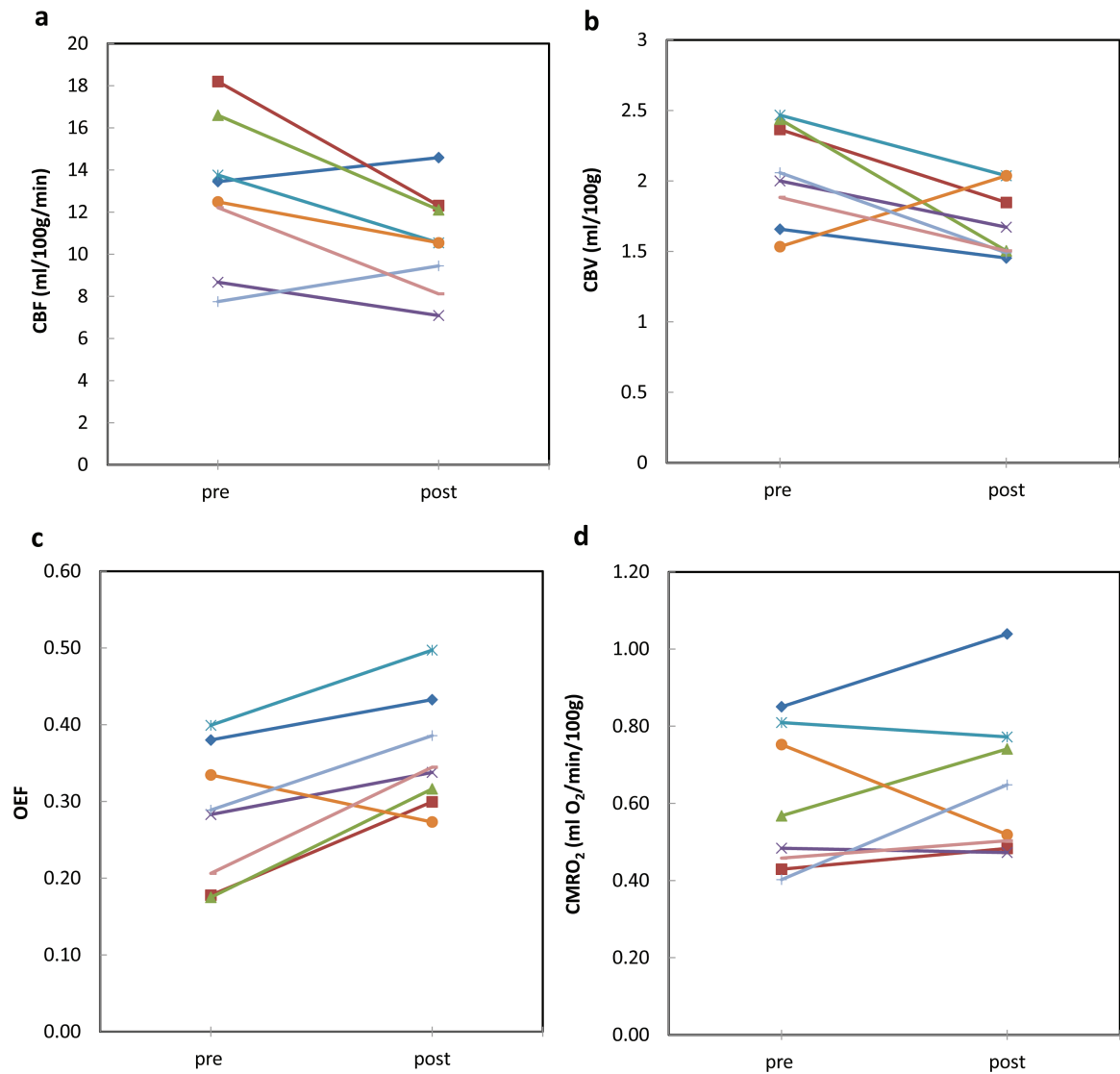


Figure 1. Individual values of pre and post single indomethacin treatment of PDA for (a) cerebral blood flow (CBF), (b) cerebral blood volume (CBV), (c) oxygen extraction fraction (OEF), and (d) the cerebral metabolic rate of oxygen (CMRO₂) (n = 8, 0.2 mg/kg). Data from each patient are represented by the same symbol and grey-scaled line in all graphs.

Discussion

The principle finding of this study was that, despite the significant reductions in CBF and CBV caused by a 30-min infusion of indomethacin, there was no change in CMRO₂. In general, this finding was expected considering that under normal conditions CMRO₂ should remain stable during relatively moderate reductions in CBF due to a compensatory increase in OEF. In this study the approximate 20% reduction in CBF was accompanied by a statistically significant increase in OEF of 29% under indomethacin. It is only when the reduction in CBF is sufficient to impede the supply of oxygen to the brain that CMRO₂ is expected to be affected [131]. These results suggest that, even at this very early age, the cerebral oxygen supply is sufficient to accommodate moderate variations in cerebral perfusion. To the best of our knowledge this study is the first to report quantitative measurements of CBF and CMRO₂ in infants obtained using ICG as a contrast agent. These results suggest that this methodology could be used for bedside assessments with other clinical conditions that have the potential to affect cerebral hemodynamics and energy metabolism.

BIBLIOGRAPHY

1. Higgins, R.D. and S. Shankaran, *Hypothermia: novel approaches for premature infants*. Early Hum Dev, 2011. **87 Suppl 1**: p. S17-8.
2. Vasiljevic, B., et al., *The role of oxidative stress in perinatal hypoxic-ischemic brain injury*. Srp Arh Celok Lek, 2012. **140**(1-2): p. 35-41.
3. Amato, M. and F. Donati, *Update on perinatal hypoxic insult: mechanism, diagnosis and interventions*. Eur.J Paediatr.Neurol., 2000. **4**(5): p. 203.
4. Volpe, J.J., *Neurology of the Newborn* 2001, Philadelphia: W.B. Saunders Company.
5. Eicher, D.J., et al., *Moderate hypothermia in neonatal encephalopathy: efficacy outcomes*. Pediatr Neurol, 2005. **32**(1): p. 11-7.
6. Gluckman, P.D., et al., *Selective head cooling with mild systemic hypothermia after neonatal encephalopathy: multicentre randomised trial*. Lancet, 2005. **365**(9460): p. 663-70.
7. Bennet, L., L. Booth, and A.J. Gunn, *Potential biomarkers for hypoxic-ischemic encephalopathy*. Semin Fetal Neonatal Med, 2010. **15**(5): p. 253-60.
8. Guo, M.F., J.Z. Yu, and C.G. Ma, *Mechanisms related to neuron injury and death in cerebral hypoxic ischaemia*. Folia Neuropathol, 2011. **49**(2): p. 78-87.
9. Ment, L.R., et al., *Practice parameter: neuroimaging of the neonate: report of the Quality Standards Subcommittee of the American Academy of Neurology and the Practice Committee of the Child Neurology Society*. Neurology, 2002. **58**(12): p. 1726.
10. Thacker, S.B., D. Stroup, and M. Chang, *Continuous electronic heart rate monitoring for fetal assessment during labor*. Cochrane Database Syst Rev, 2001(2): p. CD000063.
11. Painter, M.J., et al., *Fetal heart rate patterns during labor: neurologic and cognitive development at six to nine years of age*. Am J Obstet Gynecol, 1988. **159**(4): p. 854-8.
12. Dammann, O. and A. Leviton, *Brain damage in preterm newborns: might enhancement of developmentally regulated endogenous protection open a door for prevention?* Pediatrics, 1999. **104**(3 Pt 1): p. 541-50.
13. Perlman, J.M., *Summary proceedings from the neurology group on hypoxic-ischemic encephalopathy*. Pediatrics, 2006. **117**(3 Pt 2): p. S28-33.
14. Blair, E., *A research definition for 'birth asphyxia'?* Dev Med Child Neurol, 1993. **35**(5): p. 449-52.
15. Penrice, J., et al., *Proton magnetic resonance spectroscopy of the brain during acute hypoxia-ischemia and delayed cerebral energy failure in the newborn piglet*. Pediatr Res, 1997. **41**(6): p. 795-802.
16. Hagberg, H., *Mitochondrial impairment in the developing brain after hypoxia-ischemia*. J Bioenerg Biomembr, 2004. **36**(4): p. 369-73.

17. Puka-Sundvall, M., et al., *Impairment of mitochondrial respiration after cerebral hypoxia-ischemia in immature rats: relationship to activation of caspase-3 and neuronal injury*. Brain Res Dev Brain Res, 2000. **125**(1-2): p. 43-50.
18. Rosenberg, A.A., et al., *Mitochondrial function after asphyxia in newborn lambs*. Stroke, 1989. **20**(5): p. 674-9.
19. Kroemer, G. and J.C. Reed, *Mitochondrial control of cell death*. Nat Med, 2000. **6**(5): p. 513-9.
20. Brown, G.C. and V. Borutaite, *Nitric oxide inhibition of mitochondrial respiration and its role in cell death*. Free Radic Biol Med, 2002. **33**(11): p. 1440-50.
21. Radi, R., et al., *Inhibition of mitochondrial electron transport by peroxynitrite*. Arch Biochem Biophys, 1994. **308**(1): p. 89-95.
22. Kristian, T., *Metabolic stages, mitochondria and calcium in hypoxic/ischemic brain damage*. Cell Calcium, 2004. **36**(3-4): p. 221-33.
23. Gilland, E., et al., *Mitochondrial function and energy metabolism after hypoxia-ischemia in the immature rat brain: involvement of NMDA-receptors*. J Cereb Blood Flow Metab, 1998. **18**(3): p. 297-304.
24. Lorek, A., et al., *Delayed ("secondary") cerebral energy failure after acute hypoxia-ischemia in the newborn piglet: continuous 48-hour studies by phosphorus magnetic resonance spectroscopy*. Pediatr Res, 1994. **36**(6): p. 699-706.
25. Grow, J. and J.D. Barks, *Pathogenesis of hypoxic-ischemic cerebral injury in the term infant: current concepts*. Clin Perinatol, 2002. **29**(4): p. 585-602, v.
26. Niatetskaya, Z.V., et al., *Mild hypoxemia during initial reperfusion alleviates the severity of secondary energy failure and protects brain in neonatal mice with hypoxic-ischemic injury*. J Cereb Blood Flow Metab, 2012. **32**(2): p. 232-41.
27. Volpe, J.J., *Neurology of the newborn*. Major Probl Clin Pediatr, 1981. **22**: p. 1-648.
28. Chau, V., K.J. Poskitt, and S.P. Miller, *Advanced neuroimaging techniques for the term newborn with encephalopathy*. Pediatr Neurol, 2009. **40**(3): p. 181-8.
29. Amess, P.N., et al., *Early brain proton magnetic resonance spectroscopy and neonatal neurology related to neurodevelopmental outcome at 1 year in term infants after presumed hypoxic-ischaemic brain injury*. Dev Med Child Neurol, 1999. **41**(7): p. 436-45.
30. Groenendaal, F., et al., *Cerebral lactate and N-acetyl-aspartate/choline ratios in asphyxiated full-term neonates demonstrated in vivo using proton magnetic resonance spectroscopy*. Pediatr Res, 1994. **35**(2): p. 148-51.
31. Penrice, J., et al., *Proton magnetic resonance spectroscopy of the brain in normal preterm and term infants, and early changes after perinatal hypoxia-ischemia*. Pediatr Res, 1996. **40**(1): p. 6-14.

32. Azzopardi, D., et al., *Prognosis of newborn infants with hypoxic-ischemic brain injury assessed by phosphorus magnetic resonance spectroscopy*. *Pediatr Res*, 1989. **25**(5): p. 445-51.
33. Toet, M.C. and P.M. Lemmers, *Brain monitoring in neonates*. *Early Hum Dev*, 2009. **85**(2): p. 77-84.
34. Hellstrom-Westas, L., I. Rosen, and N.W. Svenningsen, *Predictive value of early continuous amplitude integrated EEG recordings on outcome after severe birth asphyxia in full term infants*. *Arch Dis Child Fetal Neonatal Ed*, 1995. **72**(1): p. F34-8.
35. Klebermass, K., et al., *Evaluation of the Cerebral Function Monitor as a tool for neurophysiological surveillance in neonatal intensive care patients*. *Childs Nerv Syst*, 2001. **17**(9): p. 544-50.
36. Toet, M.C., et al., *Amplitude integrated EEG 3 and 6 hours after birth in full term neonates with hypoxic-ischaemic encephalopathy*. *Arch Dis Child Fetal Neonatal Ed*, 1999. **81**(1): p. F19-23.
37. al Naqeeb, N., et al., *Assessment of neonatal encephalopathy by amplitude-integrated electroencephalography*. *Pediatrics*, 1999. **103**(6 Pt 1): p. 1263-71.
38. Shalak, L.F., et al., *Amplitude-integrated electroencephalography coupled with an early neurologic examination enhances prediction of term infants at risk for persistent encephalopathy*. *Pediatrics*, 2003. **111**(2): p. 351-7.
39. Ong, L.C., et al., *The usefulness of early ultrasonography, electroencephalography and clinical parameters in predicting adverse outcomes in asphyxiated term infants*. *Singapore Med J*, 2009. **50**(7): p. 705-9.
40. Shankaran, S., et al., *Predictive value of an early amplitude integrated electroencephalogram and neurologic examination*. *Pediatrics*, 2011. **128**(1): p. e112-20.
41. Pezzani, C., et al., *Neonatal electroencephalography during the first twenty-four hours of life in full-term newborn infants*. *Neuropediatrics*, 1986. **17**(1): p. 11-8.
42. Jobsis, F.F., *Noninvasive, infrared monitoring of cerebral and myocardial oxygen sufficiency and circulatory parameters*. *Science*, 1977. **198**(4323): p. 1264-7.
43. Kreis, R., T. Ernst, and B.D. Ross, *Development of the human brain: in vivo quantification of metabolite and water content with proton magnetic resonance spectroscopy*. *Magn Reson Med*, 1993. **30**(4): p. 424-37.
44. Matcher, S.J., M. Cope, and D.T. Delpy, *Use of the water absorption spectrum to quantify tissue chromophore concentration changes in near-infrared spectroscopy*. *Phys Med Biol*, 1994. **39**(1): p. 177-96.
45. Matcher, S.J. and C.E. Cooper, *Absolute quantification of deoxyhaemoglobin concentration in tissue near infrared spectroscopy*. *Phys Med Biol*, 1994. **39**(8): p. 1295-312.
46. Davie, S.N. and H.P. Grocott, *Impact of extracranial contamination on regional cerebral oxygen saturation: a comparison of three cerebral oximetry technologies*. *Anesthesiology*, 2012. **116**(4): p. 834-40.

47. Petrova, A. and R. Mehta, *Near-infrared spectroscopy in the detection of regional tissue oxygenation during hypoxic events in preterm infants undergoing critical care*. *Pediatr Crit Care Med*, 2006. **7**(5): p. 449-54.
48. Duncan, A., et al., *Optical pathlength measurements on adult head, calf and forearm and the head of the newborn infant using phase resolved optical spectroscopy*. *Phys Med Biol*, 1995. **40**(2): p. 295-304.
49. Kety, S.S. and C.F. Schmidt, *The Nitrous Oxide Method for the Quantitative Determination of Cerebral Blood Flow in Man: Theory, Procedure and Normal Values*. *J Clin Invest*, 1948. **27**(4): p. 476-83.
50. Brun, N.C., et al., *Near-infrared monitoring of cerebral tissue oxygen saturation and blood volume in newborn piglets*. *Am J Physiol*, 1997. **273**(2 Pt 2): p. H682-6.
51. Bucher, H.U., et al., *Comparison between near infrared spectroscopy and ¹³³Xenon clearance for estimation of cerebral blood flow in critically ill preterm infants*. *Pediatr Res*, 1993. **33**(1): p. 56-60.
52. Edwards, A.D., et al., *Measurement of hemoglobin flow and blood flow by near-infrared spectroscopy*. *J Appl Physiol*, 1993. **75**(4): p. 1884-9.
53. Skov, L., O. Pryds, and G. Greisen, *Estimating cerebral blood flow in newborn infants: comparison of near infrared spectroscopy and ¹³³Xe clearance*. *Pediatr Res*, 1991. **30**(6): p. 570-3.
54. Colacino, J.M., B. Grubb, and F.F. Jobsis, *Infra-red technique for cerebral blood flow: comparison with ¹³³Xenon clearance*. *Neurol Res*, 1981. **3**(1): p. 17-31.
55. Mi, W.D., et al., *Possible overestimation of indocyanine green-derived plasma volume early after induction of anesthesia with propofol/fentanyl*. *Anesth Analg*, 2003. **97**(5): p. 1421-7.
56. Speich, R., et al., *Anaphylactoid reactions after indocyanine-green administration*. *Ann Intern Med*. 1988 Aug 15;109(4):345-6.
57. Garski, T.R., et al., *Adverse reactions after administration of indocyanine green*: *JAMA*. 1978 Aug 18;240(7):635.
58. Benya, R., J. Quintana, and B. Brundage, *Adverse reactions to indocyanine green: a case report and a review of the literature*. *Cathet Cardiovasc Diagn*, 1989. **17**(4): p. 231-3.
59. Anthony, M.Y., et al., *Measurement of plasma volume in neonates*. *Arch Dis Child*, 1992. **67**(1 Spec No): p. 36-40.
60. Leung, T.S., et al., *A new method for the measurement of cerebral blood volume and total circulating blood volume using near infrared spatially resolved spectroscopy and indocyanine green: application and validation in neonates*. *Pediatr Res*, 2004. **55**(1): p. 134-41.
61. Stanga, P.E., J.I. Lim, and P. Hamilton, *Indocyanine green angiography in chorioretinal diseases: indications and interpretation: an evidence-based update*. *Ophthalmology*, 2003. **110**(1): p. 15-21; quiz 22-3.
62. Hope-Ross, M., et al., *Adverse reactions due to indocyanine green*. *Ophthalmology*, 1994. **101**(3): p. 529-33.

63. Patel, J., et al., *Measurement of cerebral blood flow in newborn infants using near infrared spectroscopy with indocyanine green*. *Pediatr Res*, 1998. **43**(1): p. 34-9.
64. Meier, P. and K.L. Zierler, *On the theory of the indicator-dilution method for measurement of blood flow and volume*. *J Appl Physiol*, 1954. **6**(12): p. 731-44.
65. Nabavi, D.G., et al., *CT assessment of cerebral perfusion: experimental validation and initial clinical experience*. *Radiology*, 1999. **213**(1): p. 141-9.
66. Brown, D.W., et al., *Quantitative near infrared spectroscopy measurement of cerebral hemodynamics in newborn piglets*. *Pediatr Res*, 2002. **51**(5): p. 564-70.
67. Ostergaard, L., et al., *High resolution measurement of cerebral blood flow using intravascular tracer bolus passages. Part II: Experimental comparison and preliminary results*. *Magn Reson Med*, 1996. **36**(5): p. 726-36.
68. Brown, D.W., J. Hadway, and T.Y. Lee, *Near-infrared spectroscopy measurement of oxygen extraction fraction and cerebral metabolic rate of oxygen in newborn piglets*. *Pediatr Res*, 2003. **54**(6): p. 861-7.
69. Phelps, M.E., et al., *Validation of tomographic measurement of cerebral blood volume with C-11-labeled carboxyhemoglobin*. *J Nucl Med*, 1979. **20**(4): p. 328-34.
70. Tichauer, K.M., et al., *Measurement of cerebral oxidative metabolism with near-infrared spectroscopy: a validation study*. *J Cereb Blood Flow Metab*, 2006. **26**(5): p. 722-30.
71. Tichauer, K.M., et al., *Near-infrared spectroscopy measurements of cerebral blood flow and oxygen consumption following hypoxia-ischemia in newborn piglets*. *J Appl Physiol*, 2006. **100**(3): p. 850-7.
72. Kurth, C.D., et al., *Cerebral oxygen saturation-time threshold for hypoxic-ischemic injury in piglets*. *Anesth Analg*, 2009. **108**(4): p. 1268-77.
73. Ioroi, T., et al., *Changes in cerebral haemodynamics, regional oxygen saturation and amplitude-integrated continuous EEG during hypoxia-ischaemia and reperfusion in newborn piglets*. *Exp Brain Res*, 2002. **144**(2): p. 172-7.
74. Tichauer, K.M., et al., *Assessing the severity of perinatal hypoxia-ischemia in piglets using near-infrared spectroscopy to measure the cerebral metabolic rate of oxygen*. *Pediatr Res*, 2009. **65**(3): p. 301-6.
75. Tichauer, K.M., et al., *Cerebral metabolic rate of oxygen and amplitude-integrated electroencephalography during early reperfusion after hypoxia-ischemia in piglets*. *J Appl Physiol*, 2009. **106**(5): p. 1506-12.
76. van den Tweel, E.R., et al., *Expression of nitric oxide synthase isoforms and nitrotyrosine formation after hypoxia-ischemia in the neonatal rat brain*. *J Neuroimmunol*, 2005. **167**(1-2): p. 64-71.
77. Peeters-Scholte, C., et al., *Neuroprotection by selective nitric oxide synthase inhibition at 24 hours after perinatal hypoxia-ischemia*. *Stroke*, 2002. **33**(9): p. 2304-10.

78. Dorrepaal, C.A., et al., *Effect of post-hypoxic-ischemic inhibition of nitric oxide synthesis on cerebral blood flow, metabolism and electrocortical brain activity in newborn lambs*. Biol Neonate, 1997. **72**(4): p. 216-26.
79. Winter, J.D., et al., *Changes in cerebral oxygen consumption and high-energy phosphates during early recovery in hypoxic-ischemic piglets: a combined near-infrared and magnetic resonance spectroscopy study*. Pediatr Res, 2009. **65**(2): p. 181-7.
80. Blood, A.B., C.J. Hunter, and G.G. Power, *Adenosine mediates decreased cerebral metabolic rate and increased cerebral blood flow during acute moderate hypoxia in the near-term fetal sheep*. J Physiol, 2003. **553**(Pt 3): p. 935-45.
81. Bona, E., et al., *Neonatal cerebral hypoxia-ischemia: the effect of adenosine receptor antagonists*. Neuropharmacology, 1997. **36**(9): p. 1327-38.
82. Edwards, A.D., et al., *Cotside measurement of cerebral blood flow in ill newborn infants by near infrared spectroscopy*. Lancet, 1988. **2**(8614): p. 770-1.
83. Skov, L., et al., *Estimation of cerebral venous saturation in newborn infants by near infrared spectroscopy*. Pediatr Res, 1993. **33**(1): p. 52-5.
84. Meek, J.H., et al., *Low cerebral blood flow is a risk factor for severe intraventricular haemorrhage*. Arch Dis Child Fetal Neonatal Ed, 1999. **81**(1): p. F15-8.
85. Bellinger, D.C., et al., *Cognitive development of children following early repair of transposition of the great arteries using deep hypothermic circulatory arrest*. Pediatrics, 1991. **87**(5): p. 701-7.
86. Chakravarti, S., S. Srivastava, and A.J. Mitnacht, *Near infrared spectroscopy (NIRS) in children*. Semin Cardiothorac Vasc Anesth, 2008. **12**(1): p. 70-9.
87. Yoxall, C.W. and A.M. Weindling, *Measurement of cerebral oxygen consumption in the human neonate using near infrared spectroscopy: cerebral oxygen consumption increases with advancing gestational age*. Pediatr Res, 1998. **44**(3): p. 283-90.
88. Kissack, C.M., et al., *Cerebral fractional oxygen extraction is inversely correlated with oxygen delivery in the sick, newborn, preterm infant*. J Cereb Blood Flow Metab, 2005. **25**(5): p. 545-53.
89. Elwell, C.E., et al., *Measurement of CMRO₂ in neonates undergoing intensive care using near infrared spectroscopy*. Adv Exp Med Biol, 2005. **566**: p. 263-8.
90. Altman, D.I., et al., *Cerebral oxygen metabolism in newborns*. Pediatrics, 1993. **92**(1): p. 99-104.
91. Roche-Labarbe, N., et al., *Near-infrared spectroscopy assessment of cerebral oxygen metabolism in the developing premature brain*. J Cereb Blood Flow Metab, 2012. **32**(3): p. 481-8.
92. Lin, P.Y., et al., *Regional and Hemispheric Asymmetries of Cerebral Hemodynamic and Oxygen Metabolism in Newborns*. Cereb Cortex, 2012.

93. Chugani, H.T., *A critical period of brain development: studies of cerebral glucose utilization with PET*. Prev Med, 1998. **27**(2): p. 184-8.
94. Borch, K. and G. Greisen, *Blood flow distribution in the normal human preterm brain*. Pediatr Res, 1998. **43**(1): p. 28-33.
95. Newberg, L.A. and J.D. Michenfelder, *Cerebral protection by isoflurane during hypoxemia or ischemia*. Anesthesiology, 1983. **59**(1): p. 29-35.
96. Koeppen, M., T. Eckle, and H.K. Eltzschig, *Selective deletion of the A1 adenosine receptor abolishes heart-rate slowing effects of intravascular adenosine in vivo*. PLoS One, 2009. **4**(8): p. e6784.
97. Maynard, D., P.F. Prior, and D.F. Scott, *Device for continuous monitoring of cerebral activity in resuscitated patients*. Br Med J, 1969. **4**(5682): p. 545-6.
98. de Vries, L.S. and L. Hellstrom-Westas, *Role of cerebral function monitoring in the newborn*. Arch Dis Child Fetal Neonatal Ed, 2005. **90**(3): p. F201-7.
99. Shalak, L. and J.M. Perlman, *Hypoxic-ischemic brain injury in the term infant-current concepts*. Early Hum Dev, 2004. **80**(2): p. 125-41.
100. Winn, H.R., R. Rubio, and R.M. Berne, *Brain adenosine concentration during hypoxia in rats*. Am J Physiol, 1981. **241**(2): p. H235-42.
101. Koos, B.J., L. Kruger, and T.F. Murray, *Source of extracellular brain adenosine during hypoxia in fetal sheep*. Brain Res, 1997. **778**(2): p. 439-42.
102. Kubonoya, K., et al., *Brain temperature and metabolic responses during umbilical cord occlusion in fetal sheep*. Pflugers Arch, 1998. **436**(5): p. 667-72.
103. Hunter, C.J., A.B. Blood, and G.G. Power, *Cerebral metabolism during cord occlusion and hypoxia in the fetal sheep: a novel method of continuous measurement based on heat production*. J Physiol, 2003. **552**(Pt 1): p. 241-51.
104. Ilie, A., et al., *Endogenous activation of adenosine A(1) receptors accelerates ischemic suppression of spontaneous electrocortical activity*. J Neurophysiol, 2006. **96**(5): p. 2809-14.
105. Ilie, A., et al., *Endogenous activation of adenosine A1 receptors promotes post-ischemic electrocortical burst suppression*. Neuroscience, 2009. **159**(3): p. 1070-8.
106. Hunter, C.J., et al., *Key neuroprotective role for endogenous adenosine A1 receptor activation during asphyxia in the fetal sheep*. Stroke, 2003. **34**(9): p. 2240-5.
107. Cunha, R.A., *Neuroprotection by adenosine in the brain: From A(1) receptor activation to A (2A) receptor blockade*. Purinergic Signal, 2005. **1**(2): p. 111-34.
108. Stone, T.W., *Adenosine, neurodegeneration and neuroprotection*. Neurol Res, 2005. **27**(2): p. 161-8.
109. Halle, J.N., et al., *Enhancing adenosine A1 receptor binding reduces hypoxic-ischemic brain injury in newborn rats*. Brain Res, 1997. **759**(2): p. 309-12.
110. Jensen, E.C., et al., *Post-hypoxic hypoperfusion is associated with suppression of cerebral metabolism and increased tissue oxygenation in near-term fetal sheep*. J Physiol, 2006. **572**(Pt 1): p. 131-9.

111. Mallard, E.C., et al., *Increased vulnerability to neuronal damage after umbilical cord occlusion in fetal sheep with advancing gestation*. Am J Obstet Gynecol, 1994. **170**(1 Pt 1): p. 206-14.
112. Puka-Sundvall, M., E. Gilland, and H. Hagberg, *Cerebral hypoxia-ischemia in immature rats: involvement of mitochondrial permeability transition?* Dev Neurosci, 2001. **23**(3): p. 192-7.
113. van den Tweel, E.R., et al., *Long-term neuroprotection with 2-iminobiotin, an inhibitor of neuronal and inducible nitric oxide synthase, after cerebral hypoxia-ischemia in neonatal rats*. J Cereb Blood Flow Metab, 2005. **25**(1): p. 67-74.
114. Broome, M.R., G.L. Collingridge, and A.J. Irving, *Activation of the NO-cGMP signalling pathway depresses hippocampal synaptic transmission through an adenosine receptor-dependent mechanism*. Neuropharmacology, 1994. **33**(11): p. 1511-3.
115. Janigro, D., et al., *Adenosine-induced release of nitric oxide from cortical astrocytes*. Neuroreport, 1996. **7**(10): p. 1640-4.
116. Barth, A., et al., *Neurotoxicity in organotypic hippocampal slices mediated by adenosine analogues and nitric oxide*. Brain Res, 1997. **762**(1-2): p. 79-88.
117. Rosenberg, A.A., E. Murdaugh, and C.W. White, *The role of oxygen free radicals in postasphyxia cerebral hypoperfusion in newborn lambs*. Pediatr Res, 1989. **26**(3): p. 215-9.
118. Gunn, A.J., et al., *Dramatic neuronal rescue with prolonged selective head cooling after ischemia in fetal lambs*. J Clin Invest, 1997. **99**(2): p. 248-56.
119. Tichauer, K.M., et al., *Using near-infrared spectroscopy to measure cerebral metabolic rate of oxygen under multiple levels of arterial oxygenation in piglets*. J Appl Physiol, 2010. **109**(3): p. 878-85.
120. Qiao, M., et al., *Development of acute edema following cerebral hypoxia-ischemia in neonatal compared with juvenile rats using magnetic resonance imaging*. Pediatr Res, 2004. **55**(1): p. 101-6.
121. Laghi Pasini, F., et al., *Increase in plasma adenosine during brain ischemia in man: a study during transient ischemic attacks, and stroke*. Brain Res Bull, 2000. **51**(4): p. 327-30.
122. Schmued, L.C. and K.J. Hopkins, *Fluoro-Jade B: a high affinity fluorescent marker for the localization of neuronal degeneration*. Brain Res, 2000. **874**(2): p. 123-30.
123. Pearce, W., *Hypoxic regulation of the fetal cerebral circulation*. J Appl Physiol, 2006. **100**(2): p. 731-8.
124. Antonucci, R., et al., *Patent ductus arteriosus in the preterm infant: new insights into pathogenesis and clinical management*. J Matern Fetal Neonatal Med, 2010. **23 Suppl 3**: p. 34-7.
125. *The Vermont-Oxford Trials Network: very low birth weight outcomes for 1990. Investigators of the Vermont-Oxford Trials Network Database Project*. Pediatrics, 1993. **91**(3): p. 540-5.

126. Ellison, R.C., et al., *Evaluation of the preterm infant for patent ductus arteriosus*. Pediatrics, 1983. **71**(3): p. 364-72.
127. Cooke, L., P. Steer, and P. Woodgate, *Indomethacin for asymptomatic patent ductus arteriosus in preterm infants*. Cochrane Database Syst Rev, 2003(2): p. CD003745.
128. Ohlsson, A., R. Walia, and S.S. Shah, *Ibuprofen for the treatment of patent ductus arteriosus in preterm and/or low birth weight infants*. Cochrane Database Syst Rev, 2010(4): p. CD003481.
129. Thomas, R.L., et al., *A meta-analysis of ibuprofen versus indomethacin for closure of patent ductus arteriosus*. Eur J Pediatr, 2005. **164**(3): p. 135-40.
130. Matcher, S.J., M. Cope, and D.T. Delpy, *Use of the water absorption spectrum to quantify tissue chromophore concentration changes in near-infrared spectroscopy*. Phys.Med Biol., 1994. **39**(1): p. 177.
131. Powers, W.J., *Cerebral hemodynamics in ischemic cerebrovascular disease*. Ann Neurol, 1991. **29**(3): p. 231-40.

Curriculum Vitae

Education

Masters in Medical Biophysics, Western University, London Ontario, 2009-Current

Honors Bachelor of Medical Sciences, Western University, London Ontario, 2004-2008

Thesis Title: Investigating Adenosine's Role in Controlling the Cerebral Metabolic Rate of Oxygen following Hypoxia-Ischemia

Supervisors: Dr Keith St. Lawrence

Brief Synopsis of Research: Investigating the relationship and mechanisms controlling oxygen metabolism in the brain following hypoxic-ischemic injuries. With the use of near infrared spectroscopy and electroencephalography, oxygenation can be obtained in human and animal models. We implemented this method in piglets along with the use of a specific antagonist against adenosine which is known to suppress cerebral metabolic levels following hypoxic-ischemic injuries. We showed that adenosine is a key component in the mediation fetal hypoxic ischemic defenses, acting to decrease the metabolic oxygen rate through specific A₁ receptors. Secondly, this work has advanced the establishment of the NIRS technique as a safe and promising tool for prognosis and treatment planning of hypoxic-ischemic encephalopathy in critically ill newborns.

Academic Experience/Employment

- *UWO Research Assistant [Geography] (2010-2011)*
 - Assisted with digital database building, mass statistical organization and analyses.

- Assisted in writing progress reports and summaries for grant committee reviews.
- *UWO Teaching Assistant [Statistical Biology] (2009-2010)*
 - Assisted with marking and providing feedback on assignments.
 - Conducted lab seminars and proctored examinations.
- *UWO Research Assistant [Neuroscience] (2008-2009)*
 - Assisted with running and analyzing psychological (e.g., kinematic) or neuro-imaging (functional MRI) experiments.
 - Duties included setting up equipment, generating stimuli, testing subjects, backing up data, doing library searches, participating in psychophysical experiments, and preparing figures.
- *UWO Research Assistant [Pharmacology] (2007-2008)*
 - Worked in a laboratory that is concerned with the development of herbal products for medicinal uses. We targeted the vascular system for the action of selected herbal products with emphasis on angiogenesis, cancer, and inflammation.
 - Duties entailed, cell culturing and counting, microscopic imaging and tumor tissue sectioning and analysis, isolating macrophagic cells from various organs as well as day to day routines (i.e. chromatography, immunoassays, centrifugation etc)

Conferences and Presentations

- **London Imaging Discovery**, London, Ontario, June 27th 2012, presented poster.
- **Lawson Research Day**, London, Ontario, March 2009-2012, presented poster and oral presentation.
- **Hot Topics in Neonatology Conference**, Washington D.C., December 2010, presented poster.

Publications

- Rohit A, **Ridha Mustafa** et al. 2012. A near-infrared spectroscopy study to assess the effects of Indomethacin on cerebral blood flow and metabolic rate of oxygen in preterm infants. *Journal of Pediatric Research*. (*Submitted*)
- **Ridha Mustafa**. 2012. Investigating the mechanisms controlling cerebral energy metabolism following perinatal hypoxic-ischemic encephalopathy. *Journal of Applied Physiology*. (*In progress*)

Awards

- Second Place at the Lawson Research Day Poster Competition, London, Ontario, 2010
- Western Graduate Research Scholarship (2009-2011).
- Deans Honor List for 4 yrs UWO (2004-2008).
- Recipient of the Queen Elizabeth II Scholarship for 3 yrs UWO (2003-2006).

Professional Memberships

- The International Society for Optics and Photonics (SPIE) 2011-Current